SACLANTCEN Memorandum
SM – 152

SACLANT ASW RESEARCH CENTRE MEMORANDUM

SPATIAL-GAIN IMPROVEMENT RESULTING FROM LEFT/RIGHT DISCRIMINATING ELEMENTS OF AN UNDERWATER TOWED ARRAY

by

RONALD A. WAGSTAFF and PIETRO ZANASCA

15 SEPTEMBER 1981

NORTH ATLANTIC TREATY ORGANIZATION

LA SPEZIA, ITALY

Published by
STI

INITIAL DISTRIBUTION

	Copies
MINISTRIES OF DEFENCE	
MOD Belgium	2
DND Canada	10
CHOD Denmark	8
MOD France	8
MOD Germany	15
MOD Greece	11
MOD Italy	10
MOD Netherlands	12
CHOD Norway	10
MOD Portugal	5
MOD Turkey	5
MOD U.K.	16
SECDEF U.S.	61
NATO AUTHORITIES	
Defence Planning Committee	3
NAMILCOM	2
SACLANT	10
SACLANTREPEUR	1
CINCWESTLANT/COMOCEANLANT	1
COMIBERLANT	1
CINCEASTLANT	1
COMSUBACLANT	1
COMMAIREASTLANT	1
SACEUR	2
CINCNORTH	1
CINCSOUTH	1
COMNAVSOUTH	1
COMSTRIKFORSOUTH	1
COMEDCENT	1
COMMARAIRMED	1
CINCHAN	1

	Copies
SCNR FOR SACLANTCEN	
SCNR Belgium	1
SCNR Canada	1
SCNR Denmark	1
SCNR Germany	1
SCNR Greece	1
SCNR Italy	1
SCNR Netherlands	1
SCNR Norway	1
SCNR Portugal	1
SCNR Turkey	1
SCNR U.K.	1
SCNR U.S.	2
SECGEN Rep. SCNR	1
NAMILCOM Rep. SCNR	1
NATIONAL LIAISON OFFICERS	
NLO Canada	1
NLO Denmark	1
NLO Germany	1
NLO Italy	1
NLO U.K.	1
NLO U.S.	1
NLR TO SACLANT	
NLR Belgium	1
NLR Canada	1
NLR Denmark	1
NLR Germany	1
NLR Greece	1
NLR Italy	1
NLR Netherlands	1
NLR Norway	1
NLR Portugal	1
NLR Turkey	1
NLR UK	1
NLR US	1
Total initial distribution	236
SACLANTCEN Library	10
Stock	34
Total number of copies	280

SACLANTCEN MEMORANDUM SM-152

NORTH ATLANTIC TREATY ORGANIZATION

SACLANT ASW Research Centre
Viale San Bartolomeo 400, I-19026 San Bartolomeo (SP), Italy.

tel: national 0187 560940
international + 39 187 560940

telex: 271148 SACENT I

SPATIAL-GAIN IMPROVEMENT RESULTING FROM LEFT/RIGHT DISCRIMINATING ELEMENTS OF AN UNDERWATER TOWED ARRAY

by

Ronald A. Wagstaff and Pietro Zanasca

15 September 1981

This memorandum has been prepared within the SACLANTCEN
Underwater Research Division as part of Project 21.

O.F. HASTRUP
Division Chief

TABLE OF CONTENTS

SPATIAL-GAIN IMPROVEMENT RESULTING FROM LEFT/RIGHT DISCRIMINATING ELEMENTS OF AN UNDERWATER TOWED ARRAY

by

Ronald A. Wagstaff and Pietro Zanasca

ABSTRACT

The improvement in spatial gain of an underwater towed array as a result of left/right discriminating elements is investigated. This is accomplished by simulating the measurement of beam noise in a dynamic shipping distribution for a major ocean basin. Beam-noise measurements by a left/right discriminating array at six locations of various shipping densities are compared with the corresponding measurements by a conventional towed array. Cumulative distribution functions of the beam noise as a function of beamwidth are used as a basis for comparison. The results indicate that the additional spatial gain is non-linear with percentage of observations. It varies from about 2 dB for 80% to about 9 to 12 dB for 10% at some sites. At other sites it is considerably less and in some cases vanishes at the low percentages.

INTRODUCTION

The objective of this study is to present statistical measures of the noise field and the response of a towed line array so as to permit the evaluation of the additional achievable gain resulting from left/right discriminating sensors.

The ability to detect an acoustical signal in the underwater ambient-noise environment can be enhanced in many ways. Spectral analysis of the output of a single sensor can separate a signal line component from a broadband noise background. Joining several sensors together in an array can spatially separate the signal from the noise, giving added gain. When the array is a horizontal linear array, the separation is in the azimuthal dimension. However, as a result of the conical nature of the acoustic response of the linear array, a left/right ambiguity exists in the determination of azimuth.

Solving this problem has been the object of many analysis techniques. Most techniques involve the acquisition of data for different array orientations. This can be accomplished with a towed array but, because of the time lapse between different data sets (corresponding to different orientations), these techniques are not always successful. A more direct approach is to construct the array with directional hydrophones that can distinguish right from left. For such an array, gains would be expected as a result of reducing or eliminating the ambiguous background noise and the left/right ambiguity of the source direction.

The extremes in achievable spatial gain of an array as a result of element left/right discrimination are easily calculated. For example, if all of the noise comes from the ambiguous direction for the signal the additional spatial gain against the noise is equal to the discrimination capability (in dB) of the individual elements. If, on the other hand, the noise comes from the same direction as the signal, there is no gain. Even a "typical gain" is difficult to define, because of the number of variables and parameters involved.

One approach that can be taken when investigating the achievable spatial gain of a left/right discriminating towed line-array is to calculate measures of array performance as a function of array parameters for situations that might be considered representative, realistic, interesting, or informative. This is the approach taken herein. The HANC (Horizontal Ambient-Noise Calculator) ambient-noise model, at present on the SACLANTCEN UNIVAC 1106, was used to generate measures of noise-field statistics and array performance that could be used to evaluate the realizable gain of an array due to left/right discriminating elements. The results for six different sites are presented and discussed briefly to illustrate their utility for the evaluation of array performance.

1 MODEL

HANC is a computerized mechanism for combining shipping distributions, source-level equations, noise vertical-arrival structure, and propagation loss to produce statistical descriptions of the noise field and the response of a towed line array. When provided with ship positions, courses, and speeds, HANC can dead-reckon the ships to new positions and calculate the array responses for many time increments. The array headings may be different for each period if desired. This allows the simulation of both noise directionality measurements and beam-noise statistics by towed arrays.

Propagation loss can be input or internally calculated. The internal calculation is an equation of the form of $A + B \log R + \alpha R$, where A and B are input, R is range, and α is a frequency-dependent attenuation coefficient. When the propagation loss is obtained externally, mode theory, ray theory, or measured data may be used. The three-dimensional response of the array can be calculated by separately specifying the vertical-arrival structure of the noise, transforming the spherical coordinate system to a conical one, and then integrating across the conical beam. The technique is described in <1>. The azimuth space may be divided into many sectors to accommodate differences in propagation characteristics along different azimuths. The sensitivity of the results to the form of the propagation-loss calculation, the vertical-arrival structure of the noise field, and the tilt of the array is addressed in Appendix A.

An additional capability that has been completed but is still being tested is the storage and use of pressure amplitudes and phases of each mode versus range and depth. This allows the calculation of array response to shipping noise by addition of the complex pressures at all elements due to each mode separately. The different modal contributions can then be combined either coherently or incoherently. With this feature, HANC can simulate measurements by an arbitrary array in shallow water and facilitate studies involving conventional and non-conventional beamforming techniques.

In the present study the propagation loss was calculated internally. The values of A and B were 69 dB and 15 dB respectively. The loss was assumed not to vary with azimuth. The noise was assumed to be concentrated between 15° and 30° from the horizontal and the array was assumed to be tilted by 6°. Although attempts are always made to tow arrays horizontally, in practice this seldom happens. The shipping distribution for the northwest Indian Ocean was used because of its availability <2>. This distribution consists of a computer-accessible data-file that contains the type, course, speed, and length of approximately 1500 ships. The type is important because tankers on north-bound courses are assumed to be empty and riding high in the water. The surface decoupling for these ships would be greater than for those on south-bound courses heading away from oil ports and presumably loaded. The course and speed are used in dead-reckoning. Speed and length are used in source-level calculations. Figure 1 plots the shipping distribution for time zero. Also included in this figure are the six locations selected for the array-response calculations used in this study.

2 APPROACH

The six sites illustrated in Fig. 1 were chosen for this study because they represent a variety of situations ranging from extremely dense shipping along all azimuths at Site 1 to no nearby shipping at Site 3. Site 2 has dense shipping in three of the four quadrants and Site 4 has ships occasionally to the south, frequently to the north, and always to the northwest and southeast. Site 6 has the shipping predominantly in the northeast half-space and Site 5 is in the middle of a dense shipping lane.

Noise measurements by a towed array were simulated at each site by using the capability in HANC to deadreckon the ships in the shipping distribution and calculate the array response. The measurements were made at 90 min intervals on fifteen different array headings distributed non-uniformly about the compass. This is the procedure normally followed in making ambient noise measurements with the towed array. Data for different headings facilitates ambiguity resolution and provides a more meaningful assessment of the beam noise spatial statistics.

Figure 2 illustrates the output of HANC for the fifteen time periods at Site 5. The noise fields are plotted in the left-hand column. The "spike" pattern is a result of the one-degree resolution of the calculated field. All of the ships in a sector of one-degree width contribute to the level of the spike in that direction. The smooth curve is the per-degree output level of an unambiguous beam five degrees wide between half-power points and sidelobes uniformly suppressed by 26 dB. This curve helps the eye to perceive the directionality in the field more readily than do the spikes. However, the distribution of spikes is probably closer to what really exists in the ambient-noise environment. The smoothed plot is indicative of the spatial smoothing done by an array with an unambiguous beam.

The right-hand column of Fig. 2 contains polar plots of the output-beam noise levels for a towed array. The two curves on each plot are for a left/right discriminating array superimposed on the corresponding output for a conventional towed array. The pattern for the latter is symmetric about the array heading arrow as a result of the left/right ambiguity. The

left-hand side of the left/right discriminating array is absent, since it was suppressed by 30 dB in the "measurement". The two curves have shading between them to better illustrate the differences.

Cumulative distribution functions of the noise-field azimuthal anisotropy were generated for each quadrant and for all azimuths from the "spiked" noise fields at each site. In addition, the array responses for each measurement period were used to generate azimuthal anisotropy cumulative distribution functions (AACDF) for the beam noise. The analogous AACDFs for an array of left/right discriminating elements were obtained by the same procedure but by reducing the ambiguous beam contribution by 30 dB. In this study, the noise to the left of the array was always discriminated against.

The array for which the measurement simulation was done had sufficient aperture to produce beams near broadside that had beamwidths of less than 2° between the half-power points. Results for arrays having narrower and also wider beamwidths were obtained by deconvolving the beam response from the "measured" beam noise and then passing through a filter of variable width.

Since no attempt is made to resolve ambiguities, the filter output is identical to the output of an array having the same response characteristics. In this study, both the array response and filter response were of the form $[\sin x/x]^2$ for the main lobe, with uniform sidelobes that were suppressed by 26 dB. Sensitivity to the sidelobe suppression-level was investigated by obtaining the same output at three sites for sidelobes suppressed by 18, 26 and 35 dB.

3 RESULTS AND DISCUSSION

The results of the model calculations can be reduced to a series of AACDF plots, of two different types. The plots in Fig. 3, which is an example of the first type, were generated by calculating distribution functions of the noise measured at Site 5 by an array having an unambiguous beam. The results for beamwidths ranging from 1° to 10° are included on the same graph. Lines of equal beam level connect the percentile levels for different beamwidths (or in this case sector widths). This is done for the four principle quadrants individually and for all azimuths. The five plots in Fig. 3 are the results for Site 5.

AACDF plots such as those in Fig. 3 are statistical measures of the spatial granularity or azimuthal anisotropy of the noise field at a particular location. For example, the results in Fig. 3e indicate that 30% of the observations of the total noise in a 4° sector of arbitrary orientation will be less than 59 dB and that 80% will be less than 71 dB. In a sector of 8° width the corresponding numbers for the total noise are 67 dB and 74 dB respectively, but are 71 dB and 76 dB respectively for noise in the northeast quadrant (Fig. 3a). The significant differences between the AACDFs for the various quadrants suggest that the noise field possesses a significant persistent directional bias to the northeast-southwest [(the first (Fig. 3a) and third (Fig. 3c) quadrants show higher levels]. This is verified by the directionality pattern for this site, which is shown, together with the directionality patterns for the other five sites, in Appendix B.

The AACDF plots of the noise field, such as those in Fig. 3, can be used to estimate the beam noise distribution functions for a towed array. However, it must be kept in mind that the AACDFs for the noise field are for sectors or unambiguous beams with infinitely suppressed sidelobes. To estimate noise levels for a towed array one must include the results for quadrants in which the ambiguous beam will be and add the appropriate sidelobe contribution. The latter increases in importance as the beamwidth becomes narrower and for the lower beam-noise levels percentiles.

A slightly different form of AACDF plot (Fig. 4) applies only to line arrays. It is generated by deconvolving the beam pattern from the "measured" beam noise data for each of the fifteen measurement periods at each site. No attempt to resolve the ambiguities is made during this process. The resulting deconvolved-folded (about the array heading) noise-field data are then used to obtain equivalent beam-noise data for arrays having beamwidths ranging from 0.5° to 10°. Cumulative distribution functions of the beam noise are then calculated.

The plotted results for beam noise measured by a conventional towed array with 26 dB sidelobes at Site 5 are given in Fig. 4a. These results suggest that an array of arbitrary orientation and having a beamwidth of 4° would measure less than 68 dB for 30% of the observations and less than 74 dB for 90%.

The AACDF plot in Fig. 4b corresponds to exactly the same case except that the ambient noise on the lefthand side of the array has been suppressed by 30 dB. This has the effect of increasing the number and width of the "holes" in the noise as well as of reducing the contribution from the ambiguous beam. In this case, an array having a beamwidth of 4° would measure less than about 64.5 dB for 30% of the observations. This represents a gain due to left/right discrimination of approximately 3.5 dB. For 90% of the observations it would be 72 dB, a gain of 2 dB. Comparisons for these and other percentages indicate that the level of gain is non-linear and increases with decreasing percentage of observations.

The AACDF plots for the noise in quadrants and the total field for Sites 1,2,3,4 and 6 are presented in Figs. 5, 7, 9, 11 and 13 respectively. The corresponding AACDF plots for the array beam noise for the same sites are in Figs. 6, 8, 10, 12 and 14; the top plot (a) is for the conventional array and the bottom (b) is for the left/right discriminating array. Sidelobe suppression levels of 26 dB, vertical-arrival structure, and 6° array tilt, as previously discussed, have been used to generate these latter figures.

The AACDF plots for the noise fields at the six different sites (Figs. 3, 5, 7, 9, 11 and 13) and the corresponding AACDF plots for the towed-array beam noise (Figs. 4, 6, 8, 10, 12 and 14) characterize the spatial variability of both the noise fields and the array outputs. Just a casual glance at the figures for the array outputs indicates some differences resulting from left/right discrimination (i.e. comparing plot a with plot b in Figs. 4, 6, 8, 10, 12 and 14). A quantitative evaluation, however, is not readily obtained. This can be facilitated by plotting the differences between the two sets of curves as a function of the percent (i.e. the abscissa). When this is done for each beamwidth and averaged for each site, the results can be seen to vary significantly with site. The curves in Fig.15 are approximations for the additional spatial gain resulting from

left/right discrimination. The array headings were arbitrarily distributed about the compass and the sidelobe suppression level was 26 dB. The numbers on the curves correspond to the site numbers.

It is evident from the curves in Fig. 15 for results averaged over beamwidths from 0.5° to 10°, that the enhancement of spatial gain due to left/right discrimination is better at Sites 1, 2 and 4 than at Sites 3, 5 and 6. It increases from about 2 dB to about 9 to 12 dB at Sites 1, 2 and 4 as the percentage of observations decreases from 90% to 10%. It is very poor at Site 3, vanishing at the low percentages. The reason for this extremely poor performance may lie in the distribution of sources at this site. The majority of the noise is due to a shipping lane to the northeast. Good gain would be expected when the directional elements are discriminating against it, i.e. on a heading of 135°. Along the other headings, however, little or no noise is being discriminated against. Hence there is less advantage due to left/right discrimination at Site 3 when the array heading is arbitrary than when the array orientation can be chosen to maximize the discrimination.

An alternative approach to comparing the performance of the two types of arrays is to compare on the basis of the percent of azimuth for which the beam level will be less than a given amount. This has practical application in the sonar equation when the beam-noise level must not exceed a given amount in order to detect a target. As the percent of azimuth yielding beam-noise levels less than the critical amount increases, the likelihood of detecting the target also increases. The curves in Fig. 16 present the results for such a means of comparison for a beamwidth of 2°, arbitrary headings, and sidelobes of 26 dB. The numbers correspond to the sites. The stars and squares correspond to 20% and 40% of azimuthal coverage by the conventional towed array. For example, at Site 2 the conventional towed array will measure beam-noise levels less than 62 dB over 20% of azimuth space. For the same beam-noise level, the unambiguous array will have 42% of the azimuthal coverage of the conventional array, or 84% of azimuth space. At beam-noise levels of 66.5 dB the azimuthal coverage of the conventional array at Site 2 is 40% while it is about 2.4 times 40, or 96%, of azimuthal space for the unambiguous array. Hence, the unambiguous array would have nearly unlimited azimuthal coverage at Site 2 with beam-noise levels less than 66.5 dB, while the ambiguous array would have acceptable beam-noise levels along only 40% of azimuth space.

The poor improvement in performance at Site 3 suggested by the corresponding curve in Fig. 15 is also reflected in Fig. 16. The gain in azimuthal coverage, at this site, due to left/right discrimination is negligible compared with the improvement for other sites.

The previous AACDF figures were for arrays on arbitrary orientations. However, the ideal situation in which to take full advantage of a left/right discrimination capability is when the target is on one side of the array and the majority of the noise is on the other. In this situation, the previous figures for gain improvement would not apply: AACDFs for a single orientation would have to be generated.

The array at Site 3 on a heading of 135° was chosen to represent the situation where the majority of the noise is on one side of the array. The dense lane to the northeast is discriminated against, while the relatively sparce lane to the southwest serves as a noise background in the direction

of the target. Fifteen periods, each separated by 1½ hours, were chosen for the measurements. Polar plots of the beam noise of a conventional array (with 26 dB sidelobes) for the 15 periods are presented in Fig. 17. Superimposed on each plot is the beam noise for a left/right discriminating array with the lefthand side suppressed. The shaded area between the two curves indicates the additional gain as a function of steering angle (or beam number) resulting from suppressing lefthand noise.

The AACDF plots in Fig. 18 convey similar information to that obtained in Fig. 17 (with the exception of discrete azimuth) but in a more useable format. The plots in the left column (a, c and e) are for a conventional array at Site 3 on a heading of 135°. The plots in the right column (b, d and f) are for the left/right discriminating array (the left-hand noise suppressed by 30 dB) also on a course of 135°. The upper plots (a and b) are for a sidelobe suppression level of 18 dB, the centre plots (c and d) for 26 dB and the bottom plots (e and f) for 35 dB.

A quick comparison of the lefthand plots with those to the right indicates that, for the higher percentages of observations (righthand sides of each plot), the additional spatial gain due to left/right discrimination is about 1 dB for 18 dB sidelobes and 4 dB for both 26 and 35 dB sidelobes. It is more difficult to make such estimates for the lower percentiles (lefthand sides of each plot) due to the high density of the curves. Figure 19 presents approximate curves (obtained by averaging over all beamwidths) for the additonal spatial gain as a function of percent of observations for the three levels of sidelobe suppression. The gain increases for 26 and 35 dB sidelobe suppression levels to about 8 and 6 dB, respectively, at the lower percentages. In this case, the additional gain for 26 dB sidelobes is greater than for 35 dB sidelobes. This does not imply that it is better to have 26 dB sidelobe suppression than 35 dB. It means that the left/right discrimination is more helpful when the sidelobes are 26 dB than when they are 35 dB. This is also limited to the very low percentiles at this site. When the sidelobe suppression is poor, 18 dB for example, the additional gain due to left/right discrimination falls to nothing below about 40%. Hence it is important to maintain reasonable sidelobes (close to 26 dB) for the left/right discrimination capability in order to achieve additional gain. It does not automatically happen.

Comparisons of the two different types of arrays on the basis of area coverage for a given beamwidth (2°) and beam-noise level are given by the curves in Fig. 20. The solid curves are for a heading of 135° and three different levels of sidelobe suppression. The dashed curve is for fifteen different headings non-uniformly distributed about the compass and 26 dB sidelobe suppression. The stars and squares indicate the beam noise levels for 20 and 40 percentiles, respectively, of azimuthal coverage. The degradation in performance improvement due to left/right discrimination as a result of deterioration in sidelobe suppression level is clearly evident from these results. The advantage of maintaining the unambiguous array parallel to the nearby shipping is also evident when comparing the dashed curve for arbitrary headings with the solid one for 135° and 26 dB sidelobe suppression.

When the array must remain within a shipping lane and maintain a constant heading along the lane, the results are slightly different. An array at Site 4, on a heading of 135°, was chosen to illustrate this situation. The corresponding AACDF plots are presented in Fig. 21. Visual estimates of the

additional spatial gain in this situation, for high percentages, are about 2 dB for 18 dB sidelobes and 3 dB for 26 and 35 dB sidelobes. The corresponding curves for additional spatial gain due to left/right discrimination are given in Fig. 22. In this situation there is a substantial gain with sidelobe suppression. The additional gain improvement below 40% is about 4 dB as the sidelobe suppression increases from 26 to 35 dB, a clear indication that the spatial gain improvement is greater for greater sidelobe suppression. This is verified in the beam-noise levels: for example, for a 3° beamwidth and 26 dB sidelobes the beam-noise levels are less than 60 dB for 30% of the observations with the left/right discriminating array. The levels are 56 dB for the same case, when the sidelobes are suppressed 35 dB. For a conventional array, the corresponding beam-noise levels are 66 dB for both sidelobe suppression levels. Again, the additional gain diminishes with decreasing percentile for 18 dB sidelobe suppression.

When Figs. 19 and 22 are compared with the results for Sites 3 and 4, respectively, in Fig. 15, the differences in additional spatial gain resulting from array orientation become evident: for an arbitrary heading, the additional gain at Site 3 was extremely poor. It increased by about 6 dB at the lower percentages, when the heading was 135° and the maximum capability of the left/right discrimination was being used. At Site 4, however, there may not be an optimum heading as there is at Site 3. This is a result of being within the shipping lane rather than to one side of it as at Site 3.

The corresponding results are slightly different when the array orientation is arbitary. Figure 23 presents the AACDF plots for a conventional array on an arbitrary orientation at Site 5 (lefthand column) and for a left/right discriminating array (right-hand column) for 18 dB (top row), 26 dB (centre row), and 35 dB sidelobes (bottom row). The curves for the approximate additional spatial gain resulting from left/right discrimination when the sidelobes are suppressed 18, 26 and 35 dB, are shown in Fig. 24. For this situation, the additional spatial gain when the sidelobes are suppressed 18 dB is nearly constant at approximately 2 dB. For 26 and 35 dB sidelobe suppression the gain is non-linear and increases at the lower percentage of observations to about 4 and 8 dB, respectively, at 10%.

CONCLUSIONS

1. The additonal achievable spatial gain of a line array due to left/right discrimination depends on the noise field, the array orientation within the noise field, and the sidelobe suppression capability of the array.

2. This gain is relatively insensitive to array beamwidth. It is highly sensitive to the noise field and the orientation of the array.

3. The level of sidelobe suppression of the array is important in determining achievable additional gain resulting from left/right discrimination. For a single heading with the majority of the noise on the side being discriminated against, it ranged from 1 to 4 dB at the high percentages (80% to 90%) of observations and 0 to 8 dB at the low

percentages (10%) when the sidelobe suppression went from 18 dB to 35 dB respectively. The maximum additional gain for 35 dB sidelobe suppression level was 6 dB.

REFERENCES

1. WAGSTAFF, R.A. Horizontal directionality estimation considering array tilt and noise field vertical-arrival structure. Journal of the Acoustical Society of America 67(4), 1980: 1287-1294.

2. SOLOMON, L. Shipping distribution for the northwest Indian Ocean. Private communication, April 1978.

FIGURES

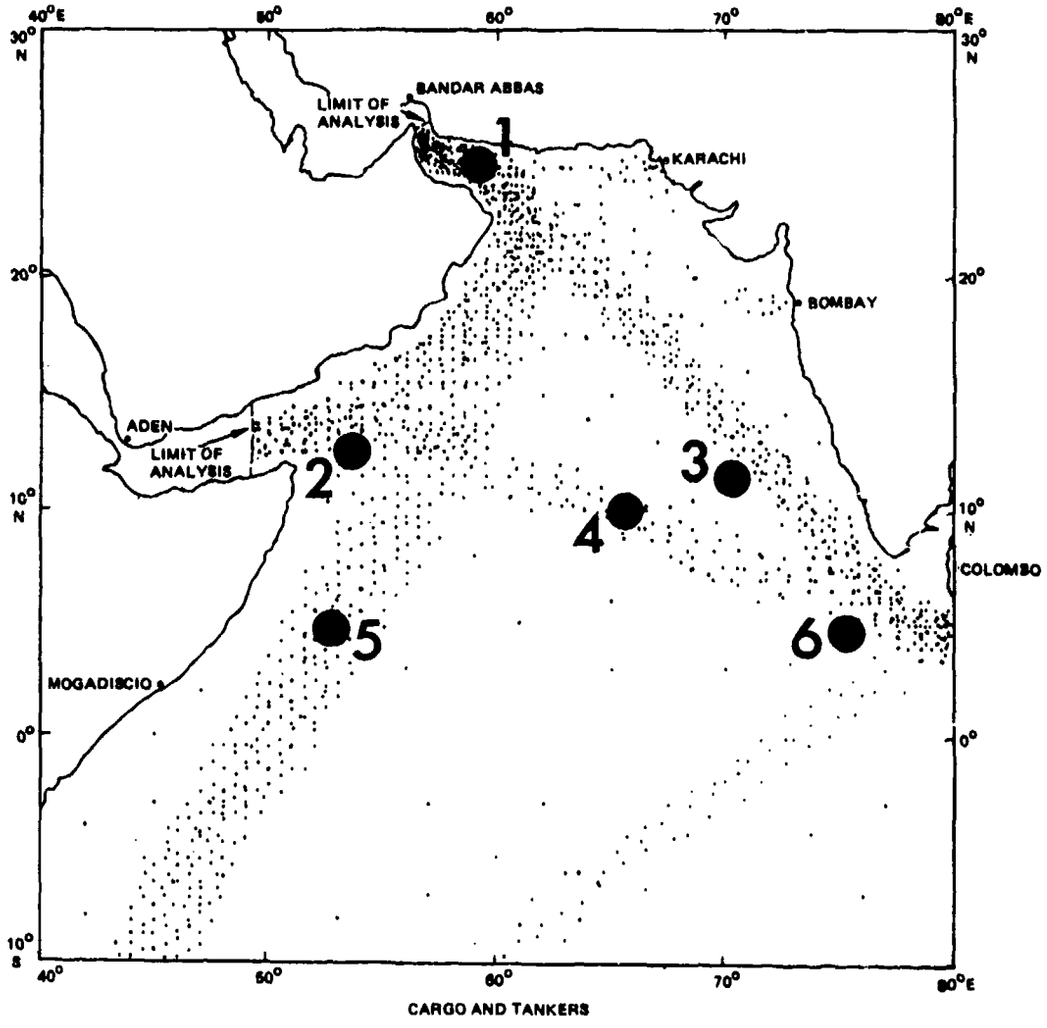

FIG. 1 SHIPPING DISTRIBUTION IN THE INDIAN OCEAN AT TIME ZERO
The numerals denote the site number and the site locations for the six sites used in this study.

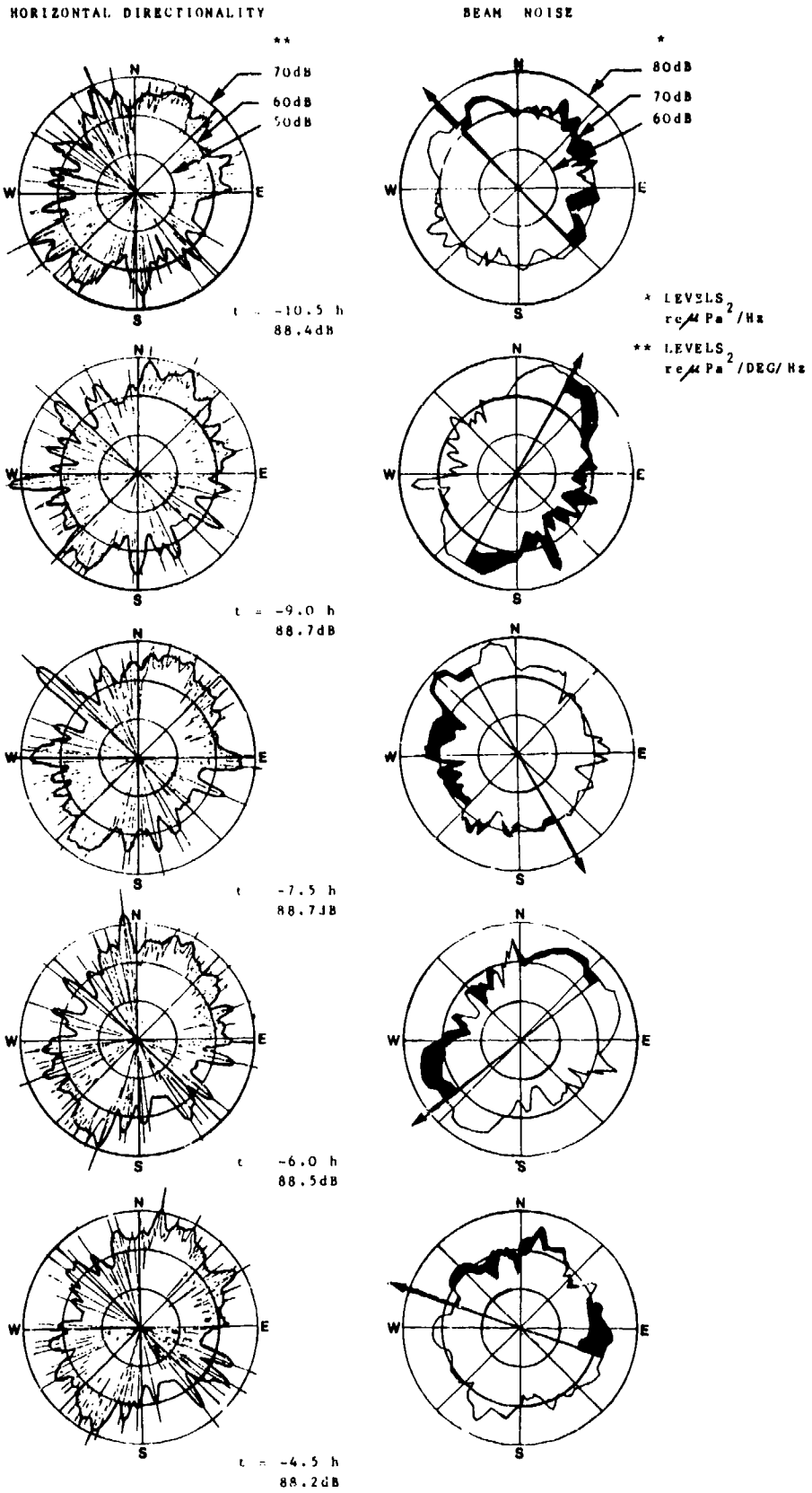

FIG. 2 SITE 5

Left-hand column ONE DEGREE RESOLUTION PLOT of the instantaneous (spikes) noisefield with superimposed unambiguous 5° beam output.

Right-hand column TOWED-ARRAY BEAM-NOISE PLOT for complete ambiguous azimuthal coverage with superimposed 30 dB left-side suppression (with shading between).

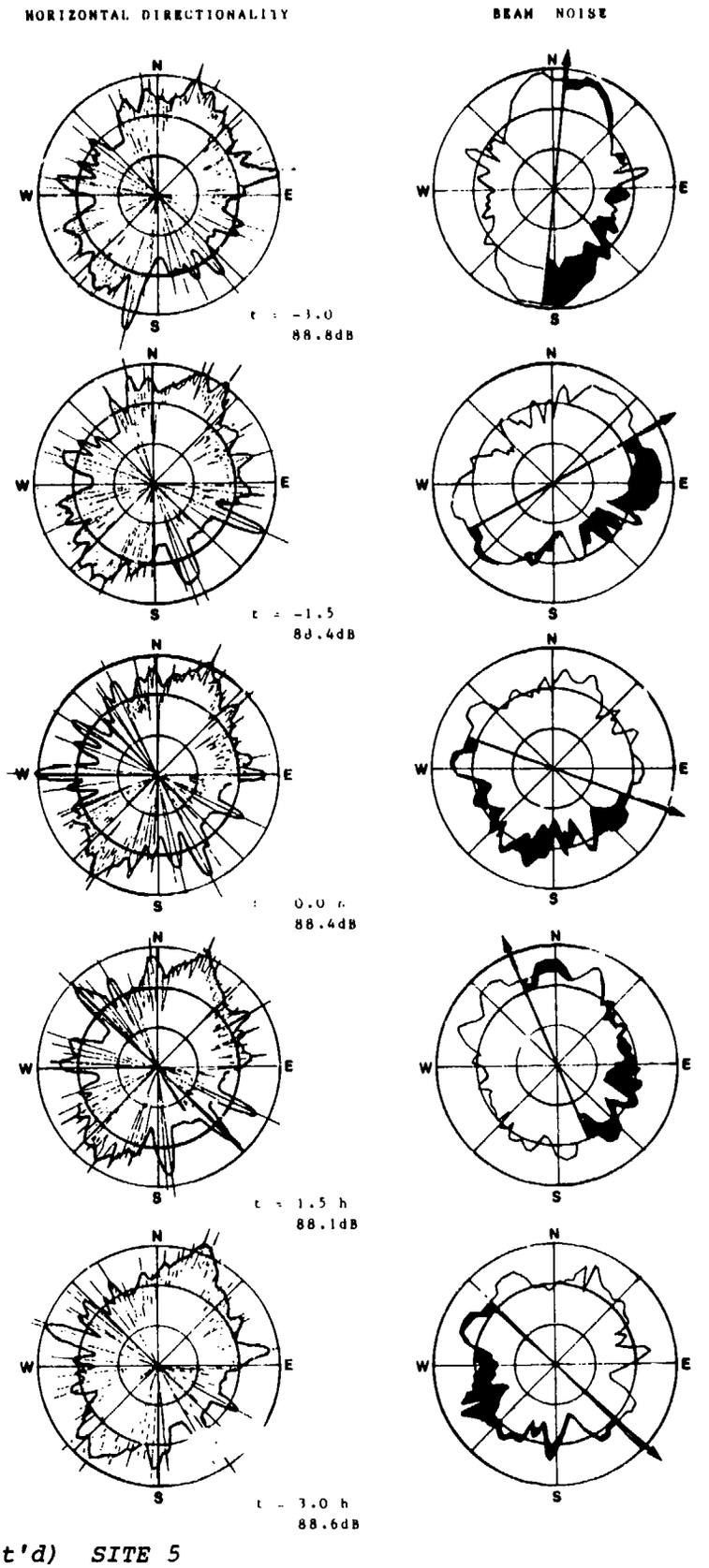

FIG. 2 (Cont'd) SITE 5

Left-hand column — *ONE DEGREE RESOLUTION PLOT of the instantaneous (spikes) noisefield with superimposed unambiguous 5° beam output.*

Right-hand column — *TOWED-ARRAY BEAM-NOISE PLOT for complete ambiguous azimuthal coverage with superimposed 30 dB left-side suppression (with shading between).*

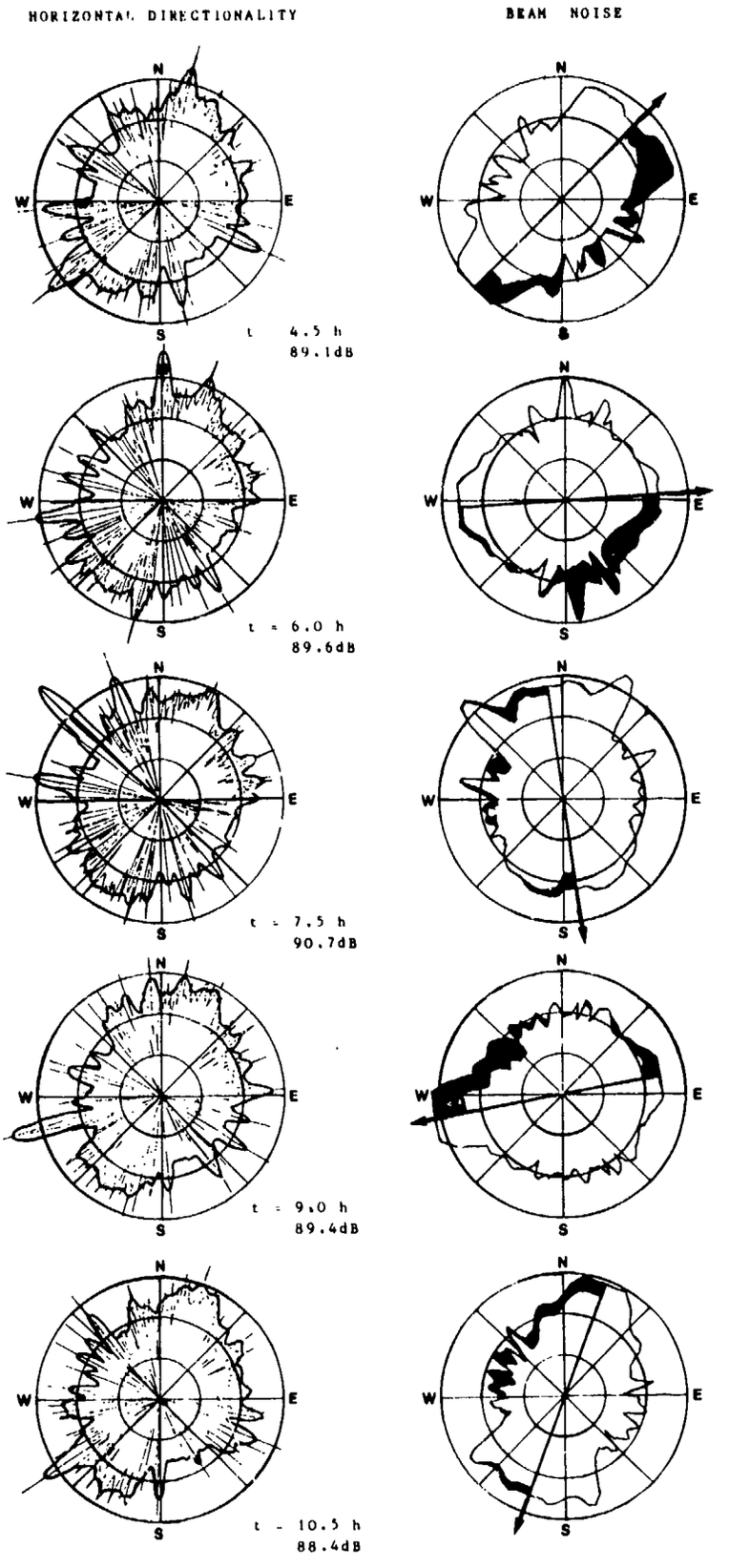

FIG. 2 (Cont'd) *SITE 5*

Left-hand column *ONE DEGREE RESOLUTION PLOT of the instantaneous (spikes) noisefield with superimposed unambiguous 5° beam output.*

Right-hand column *TOWED-ARRAY BEAM-NOISE PLOT for complete ambiguous azimuthal coverage with superimposed 30 dB left-side suppression (with shading between).*

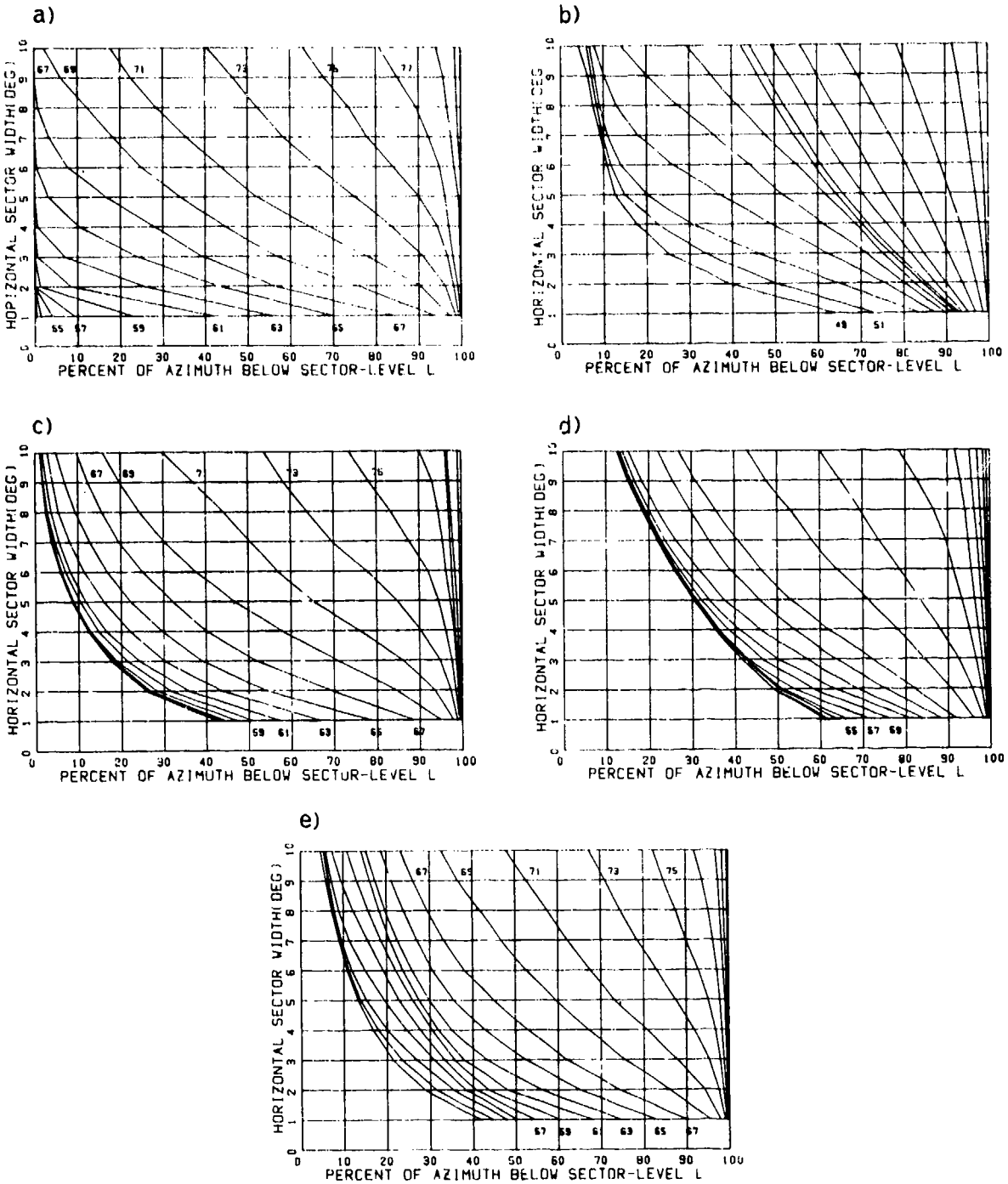

FIG. 3 SITE 5 - AACDF PLOTS OF SECTOR (OR UNAMBIGUOUS BEAM) NOISE LEVELS FOR a-d) four principal quadrants e) all azimuths Mean omnidirectional level and standard deviation are 88.8 dB and 0.65 dB respectively.

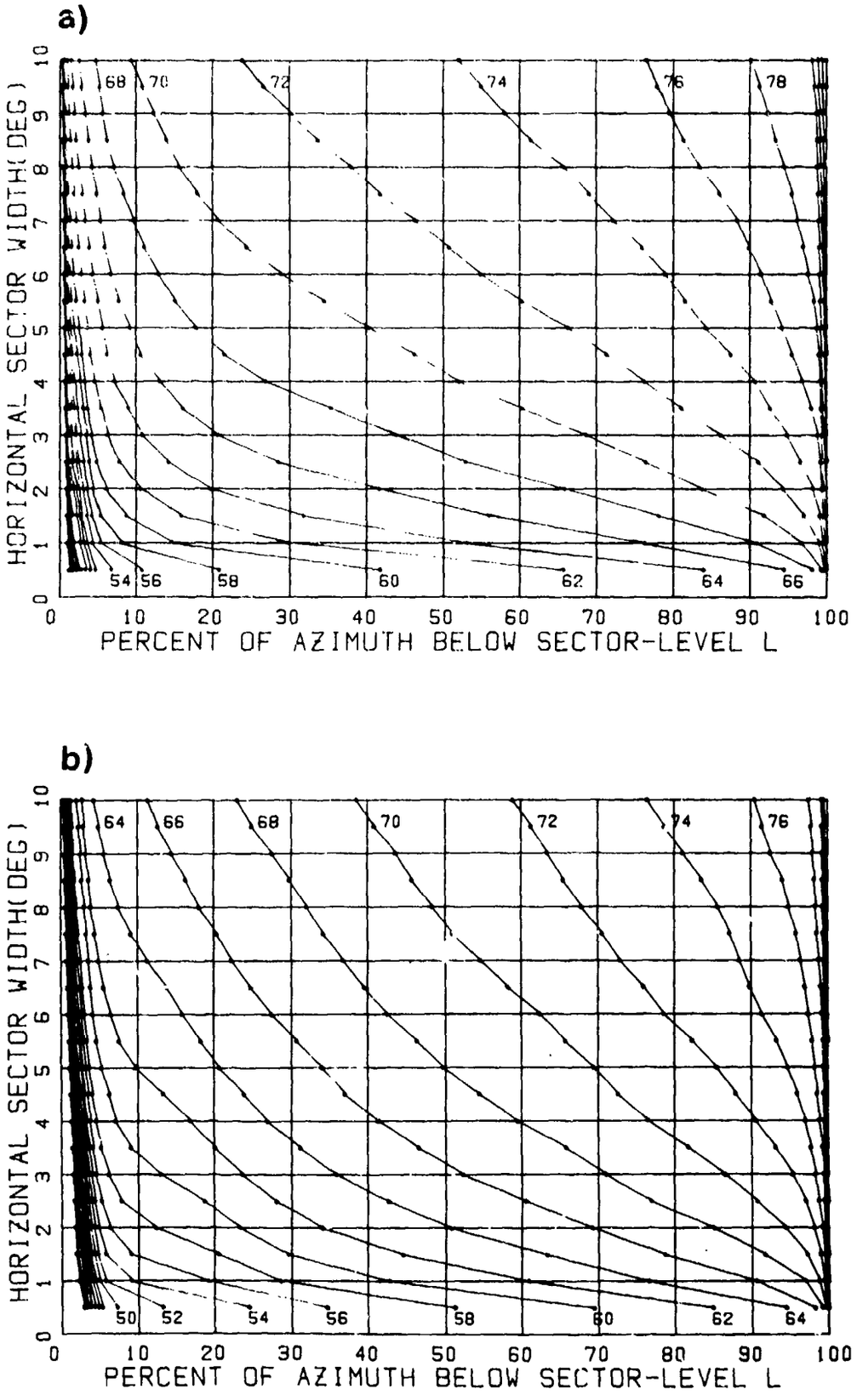

FIG. 4 SITE 5 - AACDF PLOTS OF BEAM-NOISE LEVEL
a) conventional towed array
b) same case but with the ambiguous beam suppressed by 30 dB

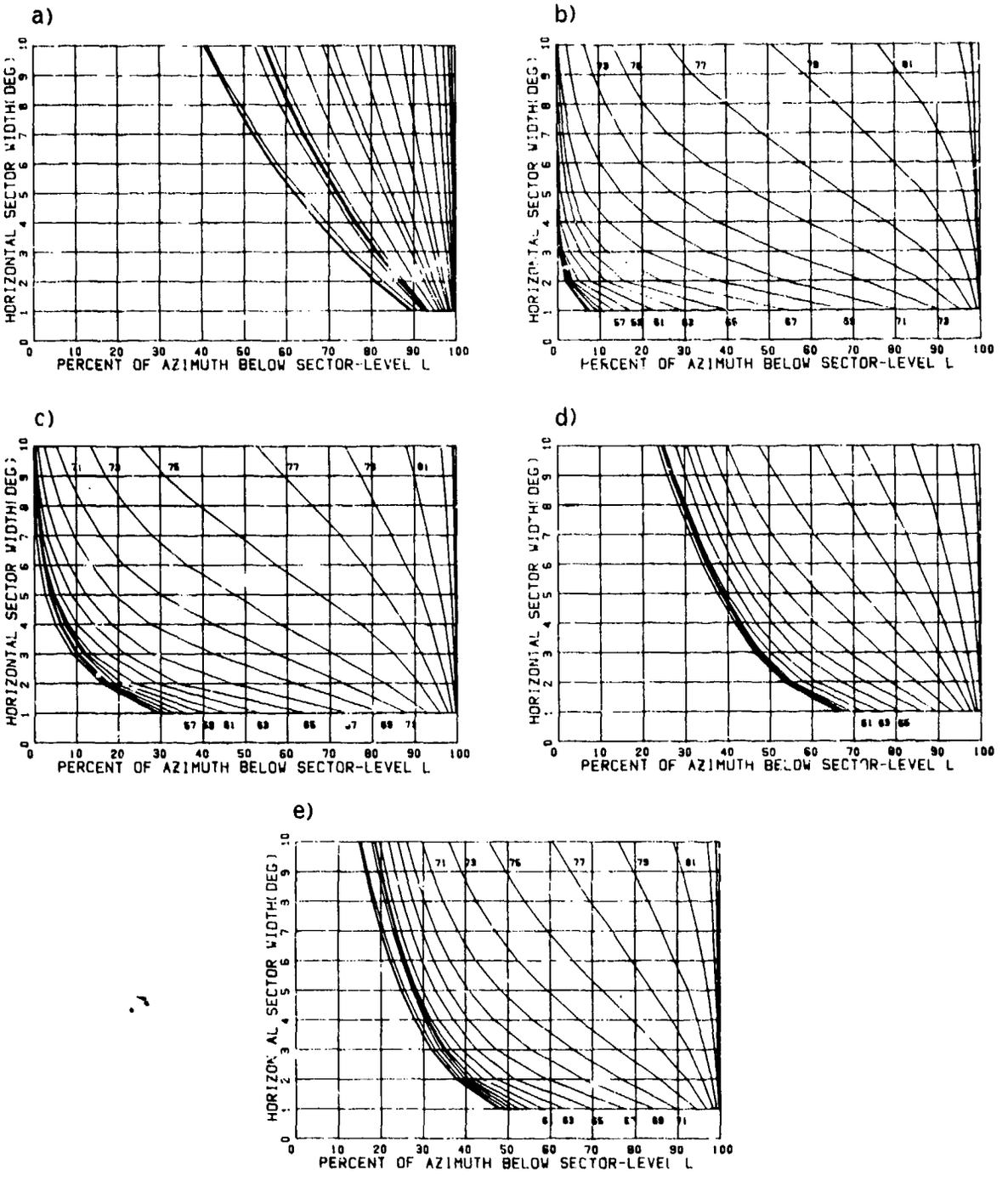

FIG. 5 SITE 1 - AACDF PLOTS OF SECTOR (OR UNAMBIGUOUS BEAM) NOISE LEVELS FOR a-d) four principal quadrants e) all azimuths Mean omnidirectional level and standard deviation are 92.7 dB and 0.92 dB respectively.

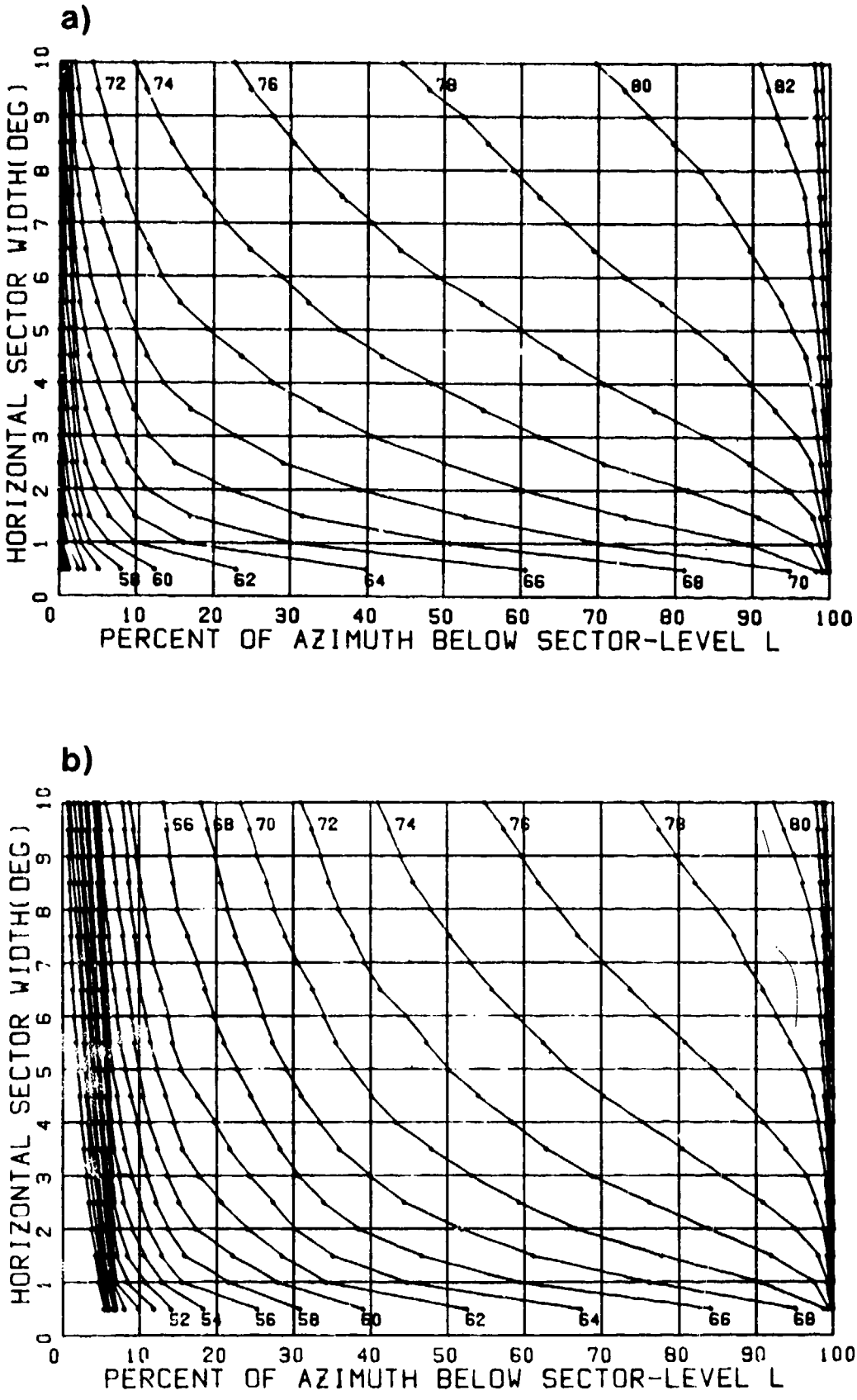

FIG. 6 SITE 1 - AACDF PLOTS OF BEAM-NOISE LEVEL

a) conventional towed array
b) same case but with the ambiguous beam suppressed by 30 dB

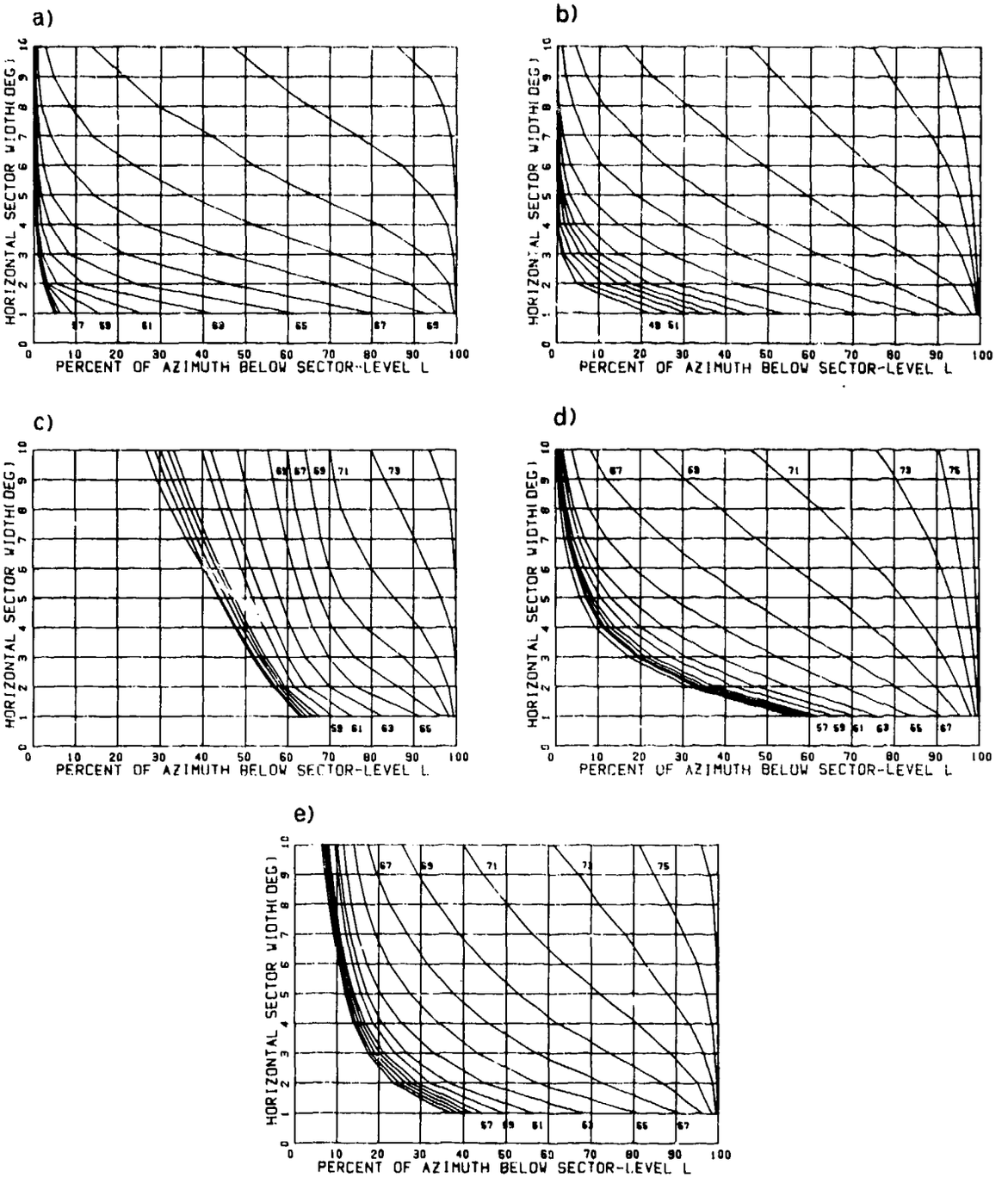

FIG. 7 SITE 2 - AACDF PLOTS OF SECTOR (OR UNAMBIGUOUS BEAM) NOISE LEVELS FOR a-d) four principal quadrants e) all azimuths Mean omnidirectional level and standard deviation are 88.3 dB and 0.12 dB respectively.

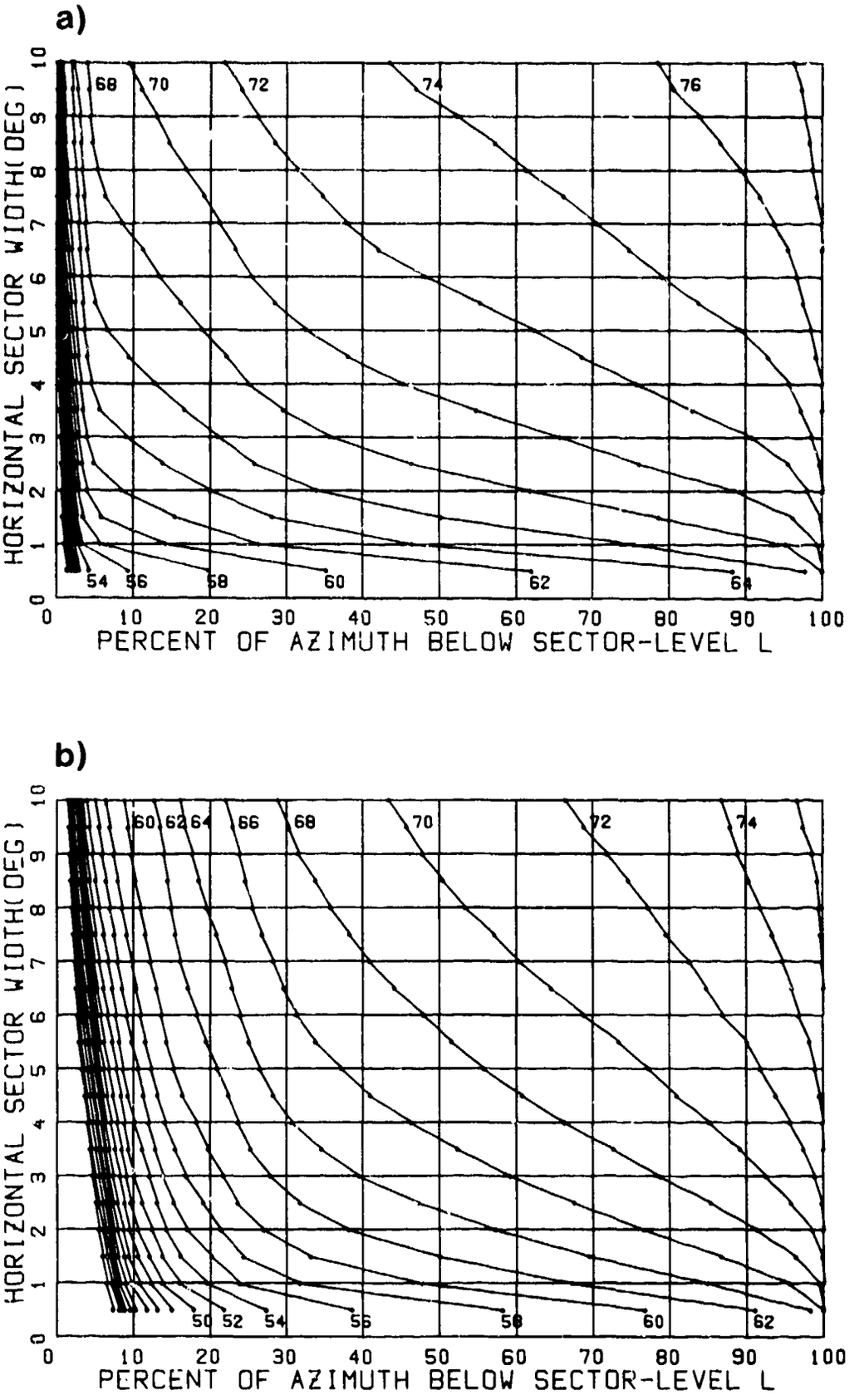

FIG. 8 SITE 2 - AACDF PLOTS OF BEAM-NOISE LEVEL
a) conventional towed array
b) same case but with the ambiguous beam suppressed by 30 dB

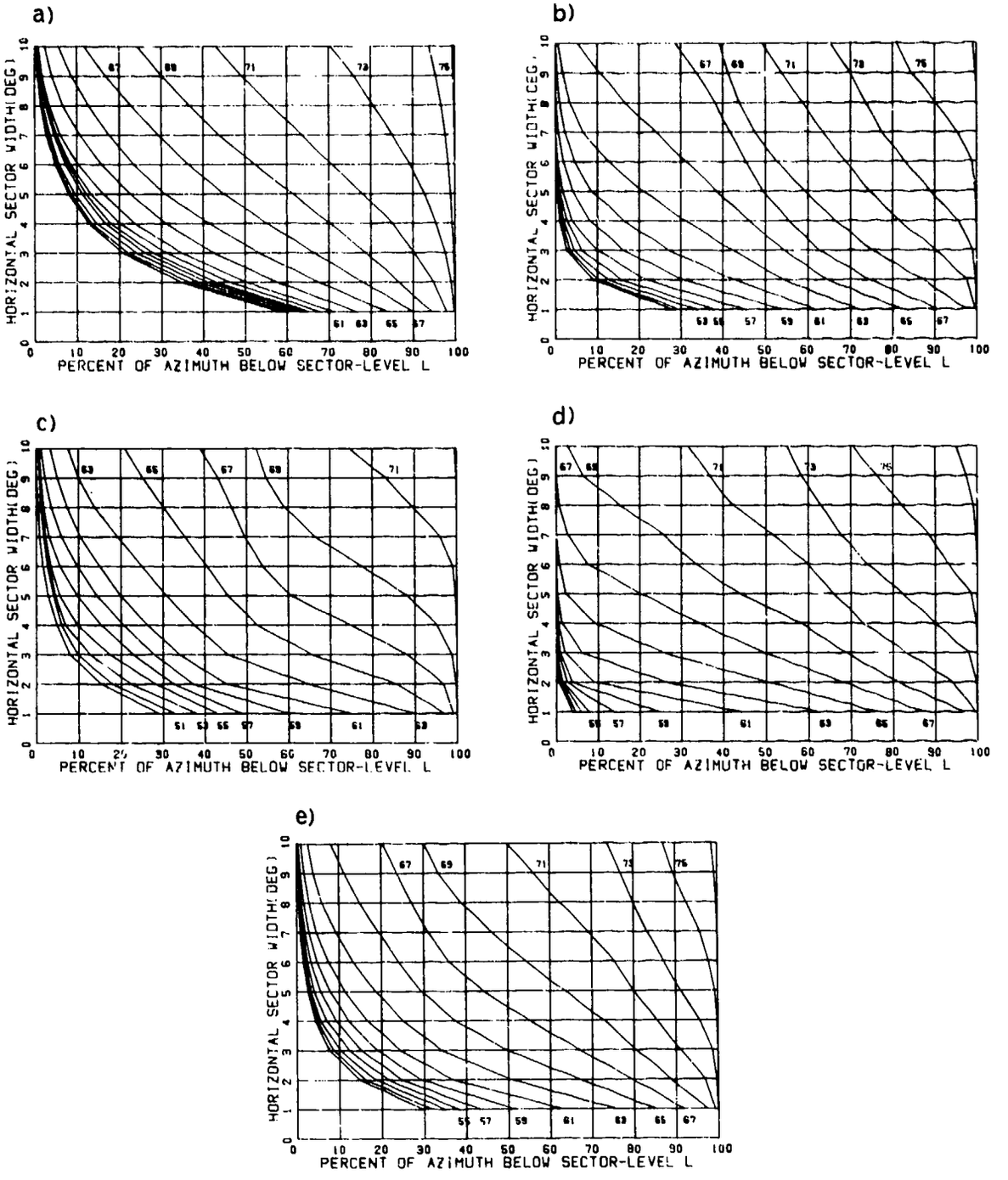

FIG. 9 SITE 3 - AACDF PLOTS OF SECTOR (OR UNAMBIGUOUS BEAM) NOISE LEVELS FOR a-d) four principal quadrants e) all azimuths Mean omnidirectional level and standard deviation are 87.6 dB and 0.1 dB respectively.

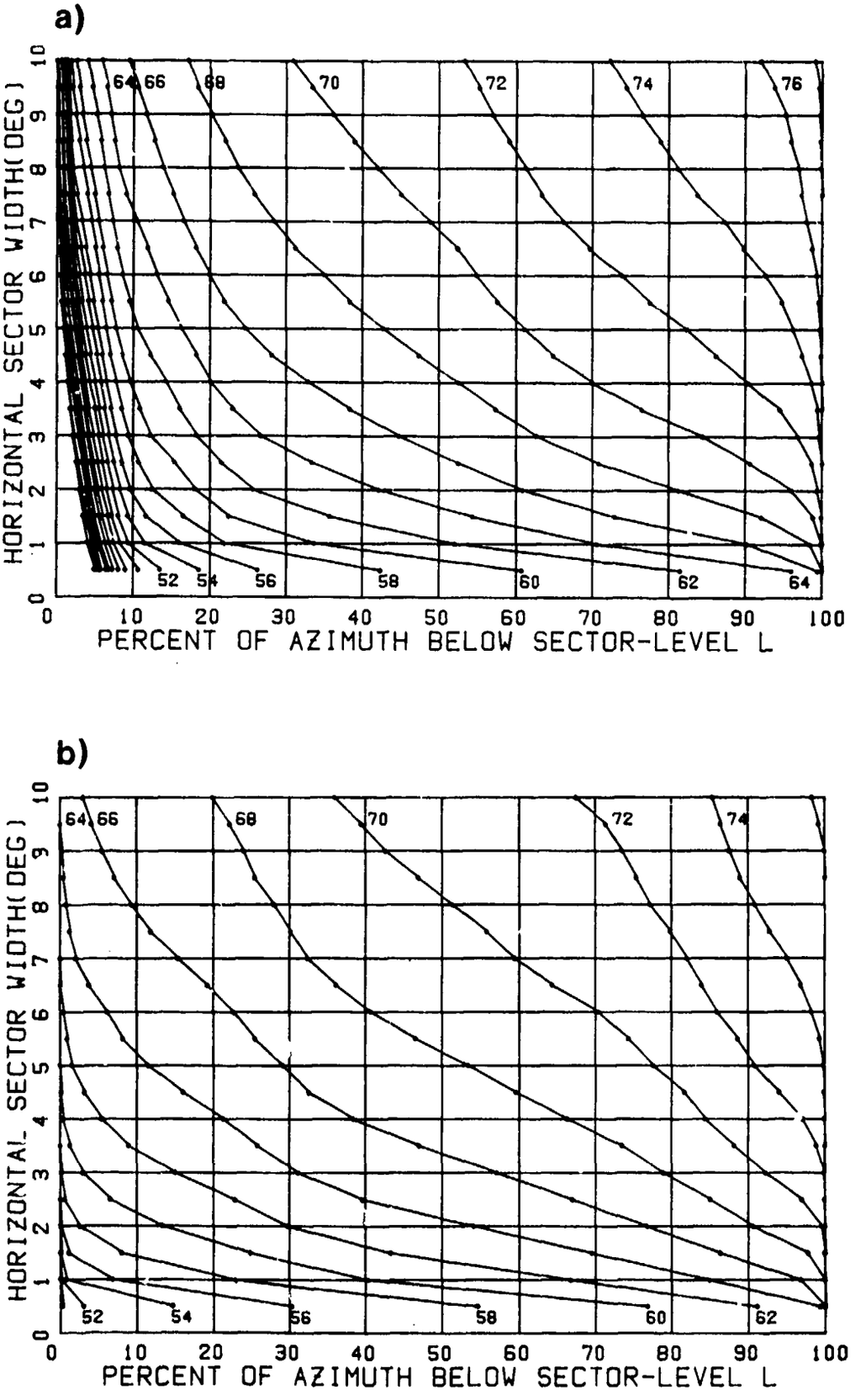

FIG. 10 SITE 3 - AACDF PLOTS OF BEAM-NOISE LEVEL
a) conventional towed array
b) same case but with the ambiguous beam suppressed by 30 dB

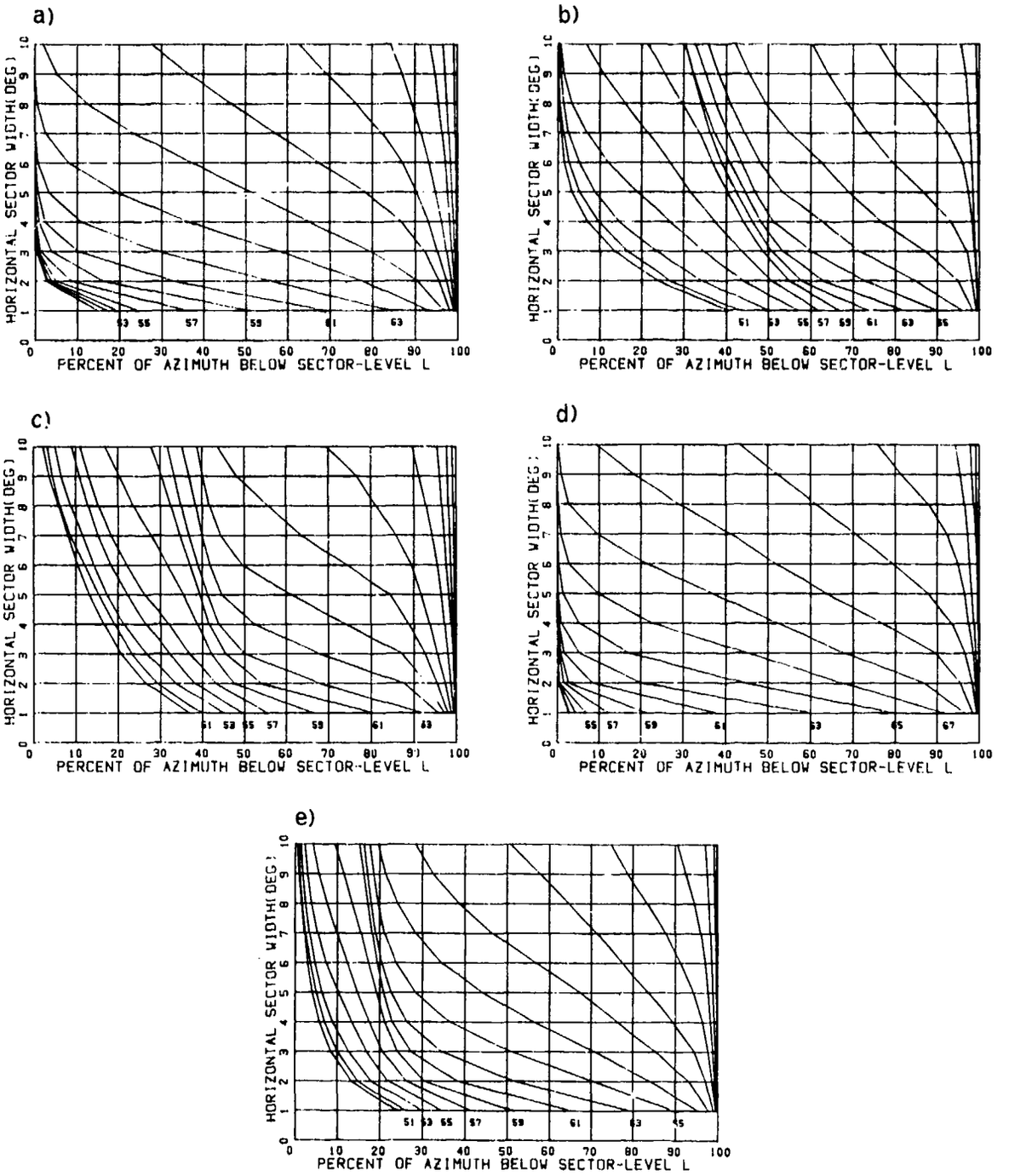

FIG. 11 SITE 4 - AACDF PLOTS OF SECTOR (OR UNAMBIGUOUS BEAM) NOISE LEVELS FOR a-d) four principal quadrants e) all azimuths Mean omnidirectional level and standard deviation are 87.6 dB and 0.54 dB respectively.

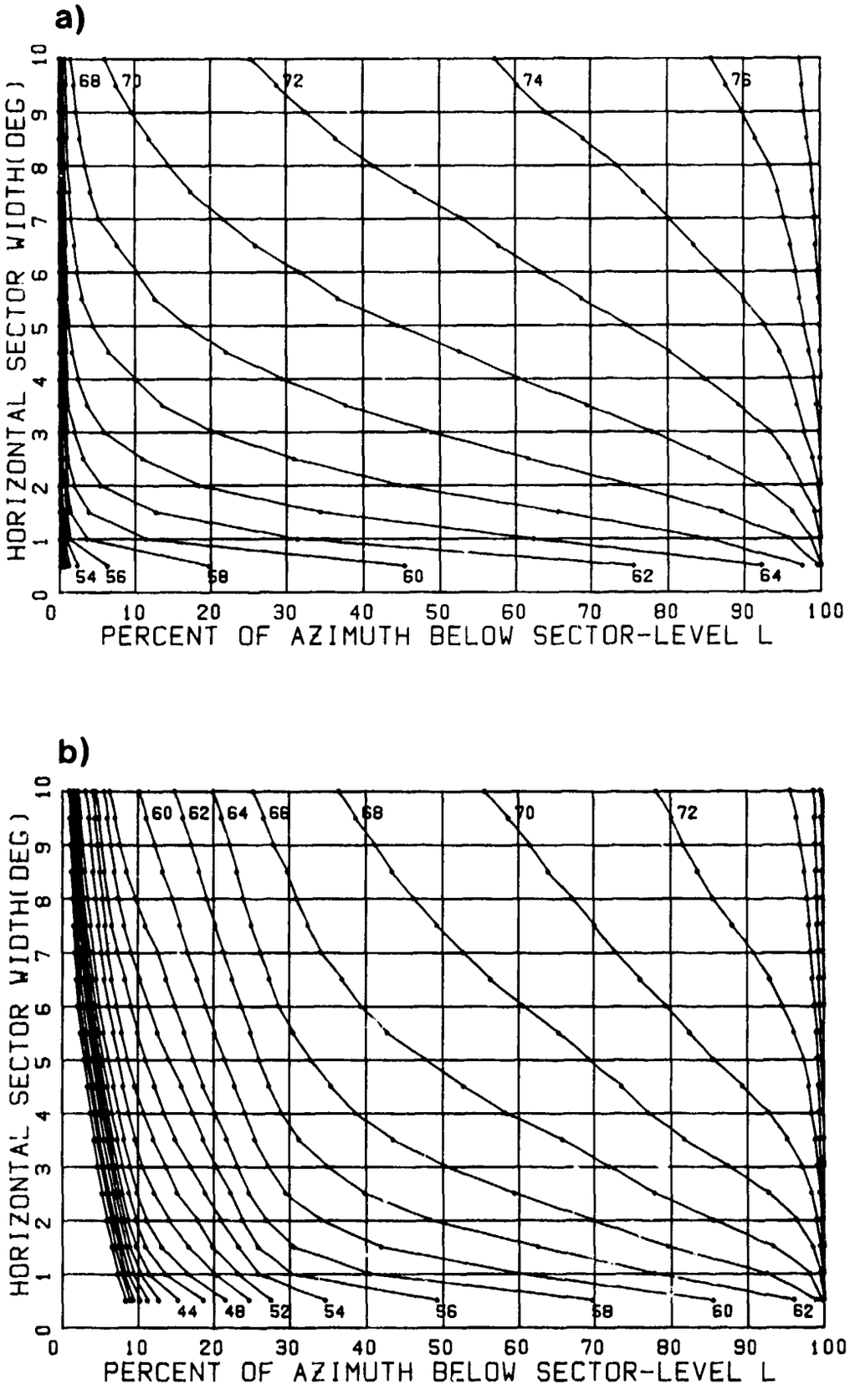

FIG. 12 SITE 4 - AACDF PLOTS OF BEAM-NOISE LEVEL
a) conventional towed array
b) same case but with the ambiguous beam suppressed by 30 dB

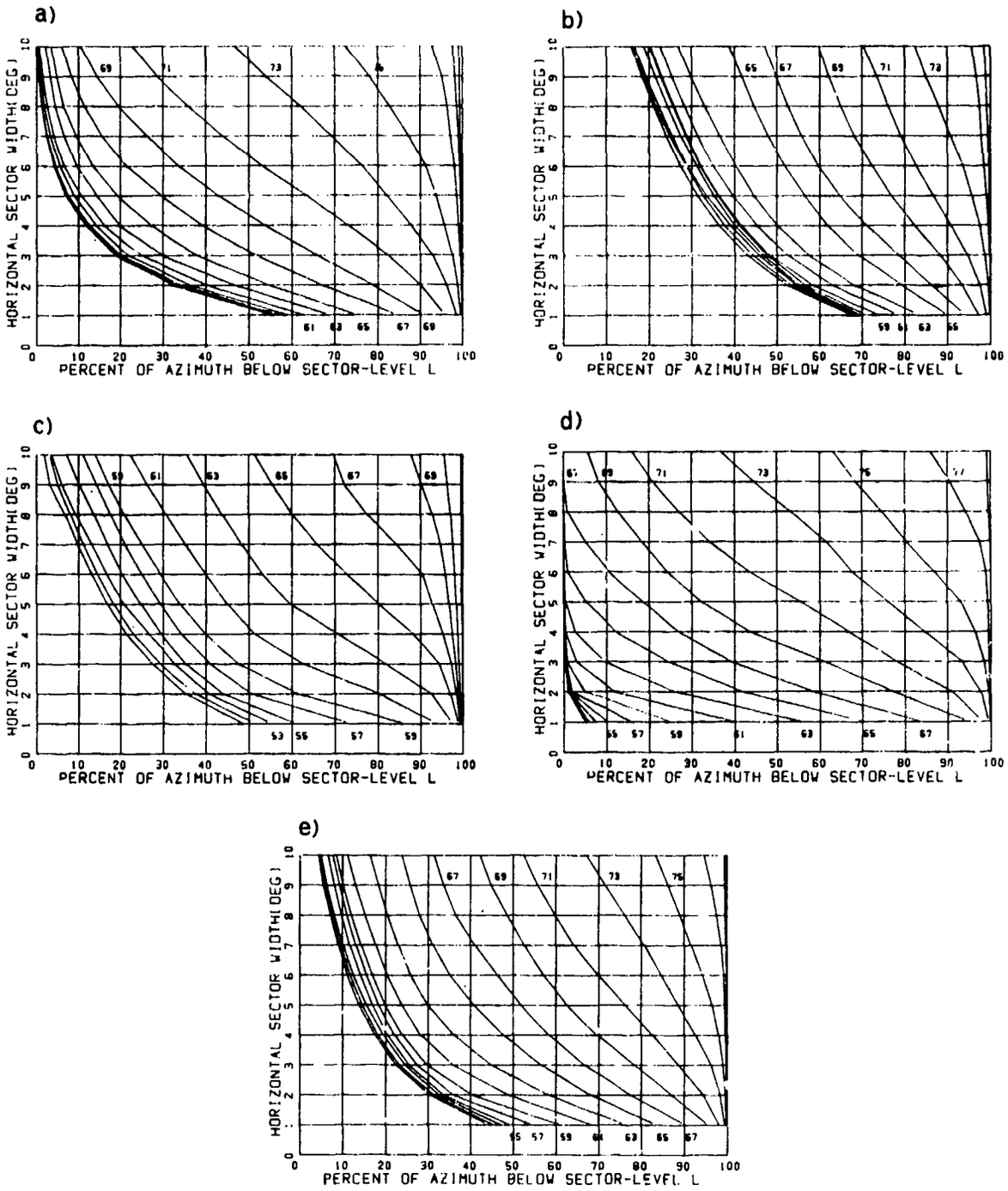

FIG. 13 SITE 6 - AACDF PLOTS OF SECTOR (OR UNAMBIGUOUS BEAM) NOISE LEVELS FOR a-d) four principal quadrants e) all azimuths Mean omnidirectional level and standard deviation are 87.3 dB and 0.23 dB respectively.

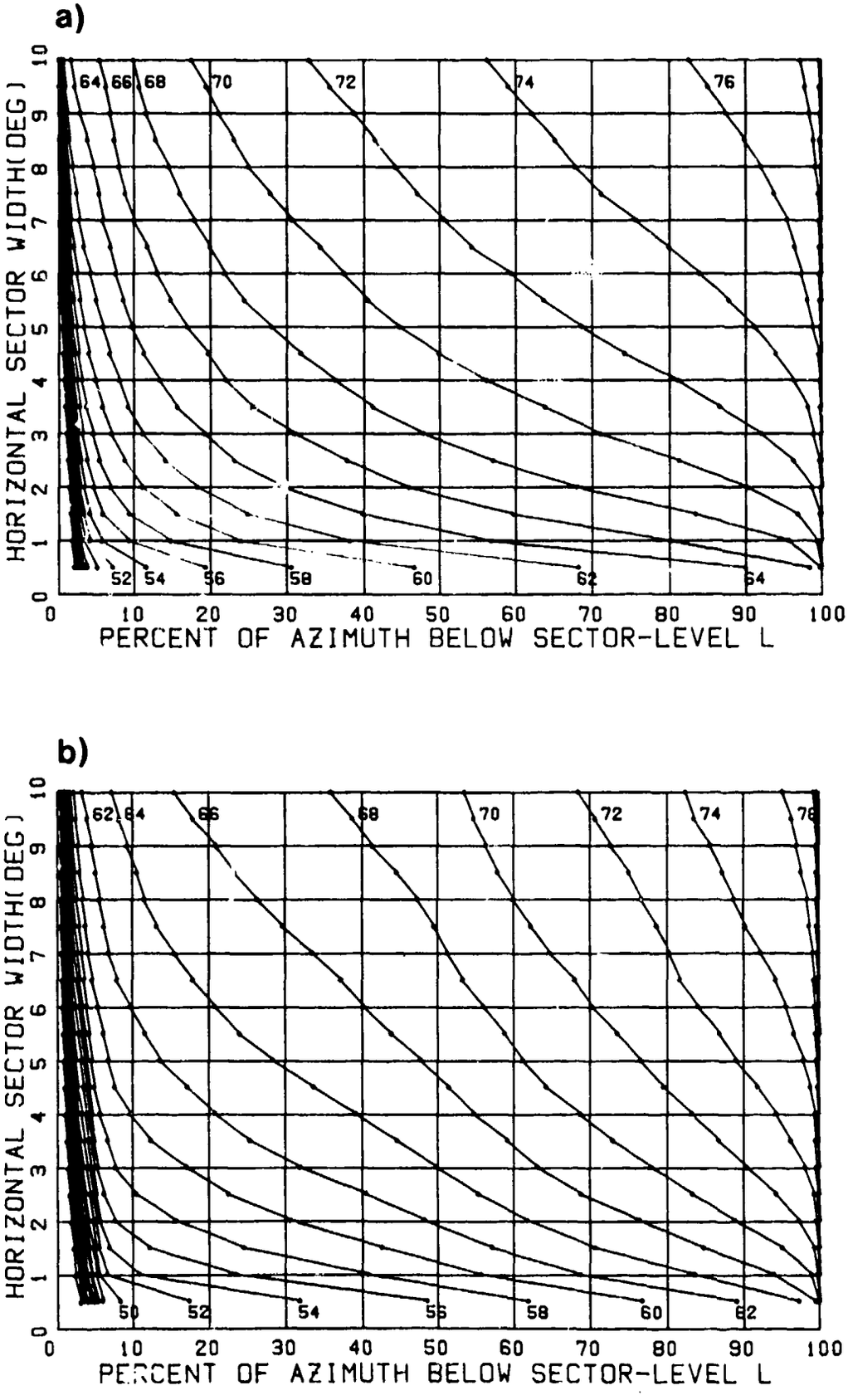

FIG. 14 SITE 6 - AACDF PLOTS OF BEAM-NOISE LEVEL
a) conventional towed array
b) same case but with the ambiguous beam suppressed by 30 dB

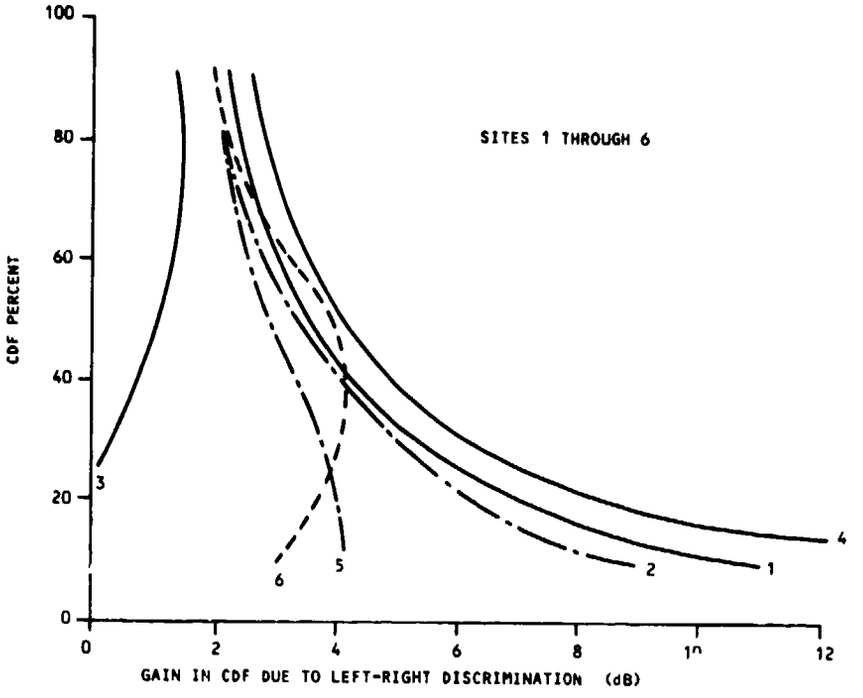

FIG. 15 SITES 1 TO 6, as numbered.
GAIN AS A FUNCTION OF PERCENTAGE OF OBSERVATIONS IN THE CUMULATIVE DISTRIBUTION FUNCTIONS (CDF) FOR TOWED-ARRAY BEAM NOISE FOR ARBITRARY ORIENTATIONS WHEN ONE (AMBIGUOUS) SIDE OF THE ARRAY IS SUPPRESSED BY 30 dB.

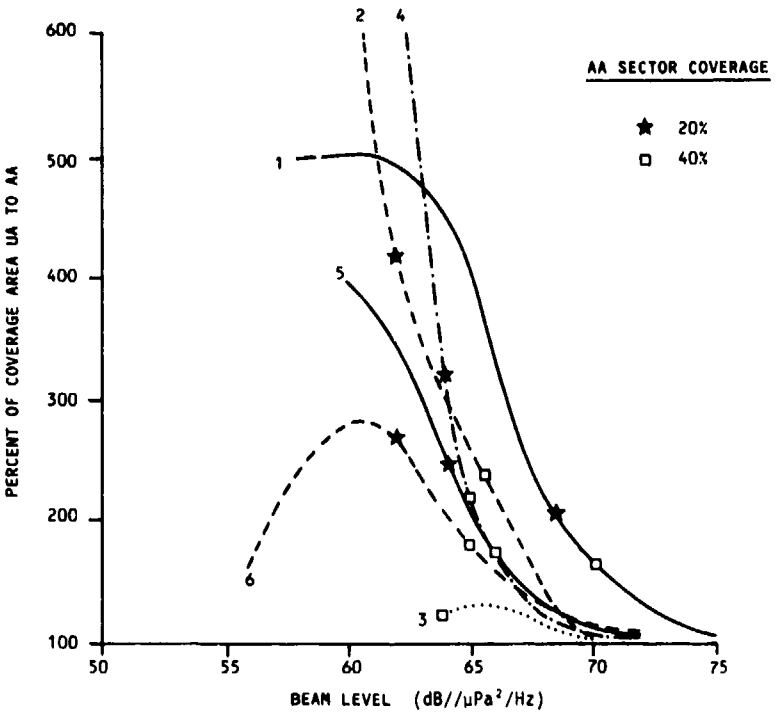

FIG. 16 SITES 1 TO 6, as numbered.
INCREASE IN PERCENT OF AREA COVERAGE IN THE CUMULATIVE DISTRIBUTION FUNCTIONS FOR AN UNAMBIGUOUS TOWED ARRAY (UA) COMPARED WITH AN AMBIGUOUS TOWED ARRAY (AA) FOR 30 dB SIDELOBE SUPPRESSION.

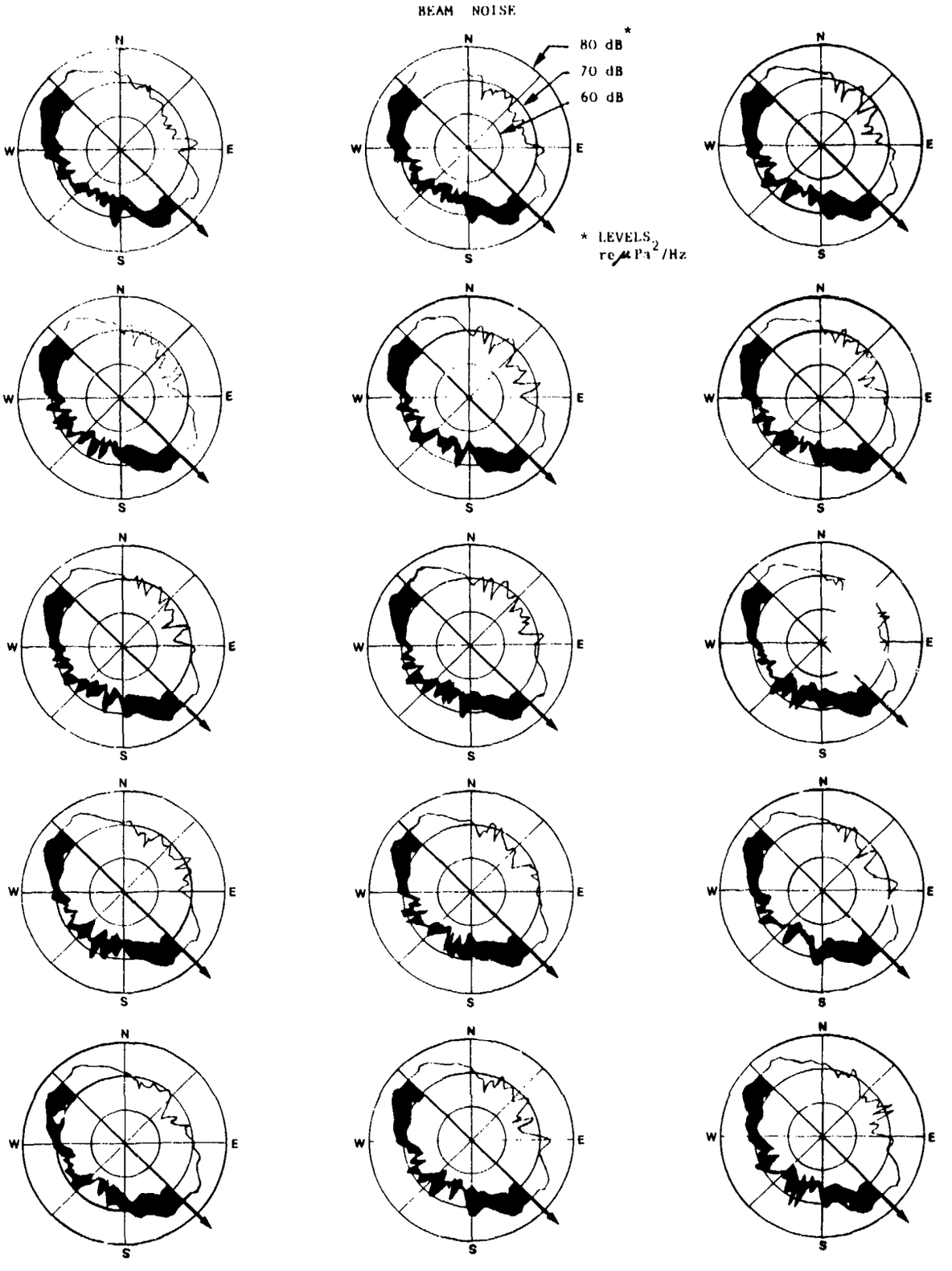

FIG. 17 SITE 3 - ARRAY BEAM NOISE LEVELS FOR A CONVENTIONAL ARRAY on a heading of 135° with superimposed beam noise levels for a left/right discriminating array (left-hand side discriminated against) with shading between. Measurement periods are separated by 1½ hours.

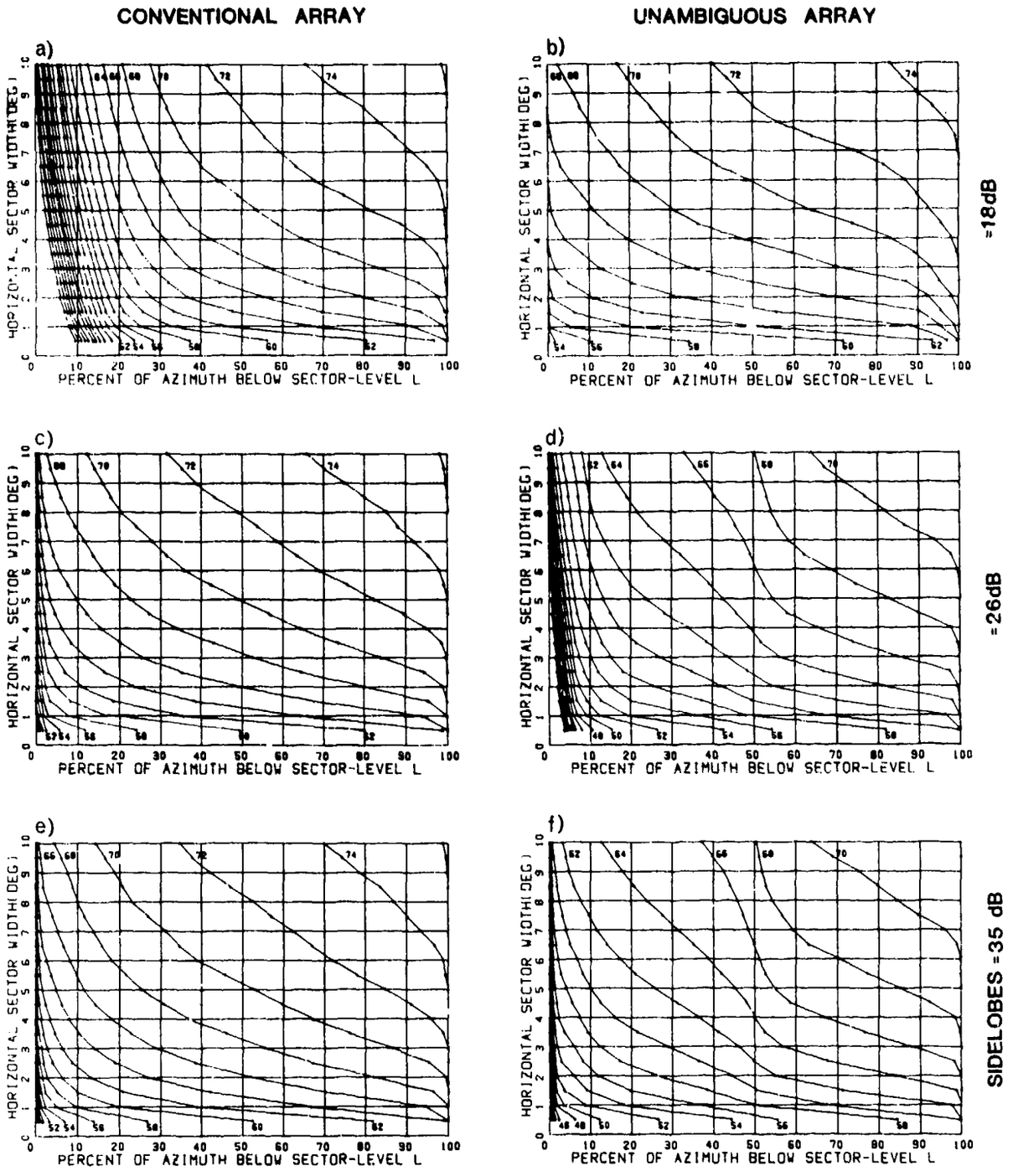

FIG. 18 SITE 3 - AACDF PLOTS
left-hand column conventional array
right-hand column left/right discriminating array with 18 dB (top row), 26 dB (centre row) and 35 dB (bottom row) sidelobe suppression. Array heading of 135°.

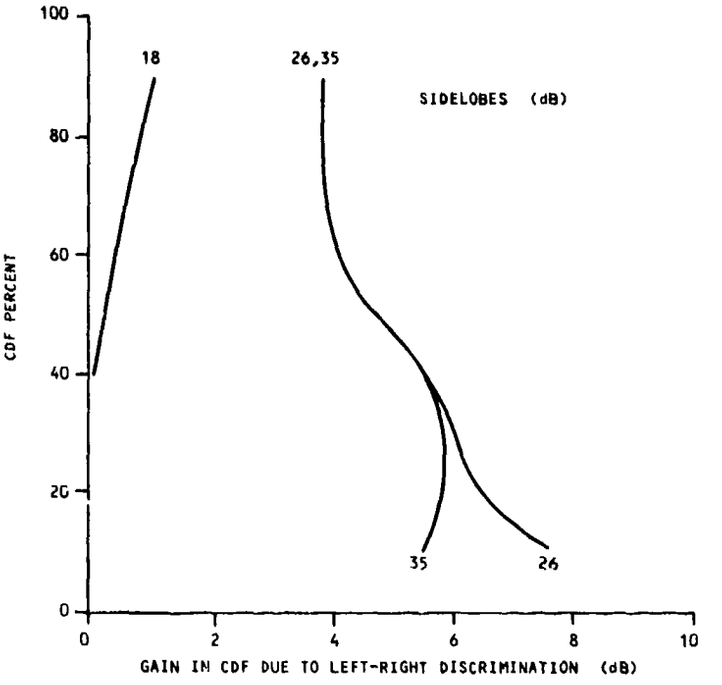

FIG. 19 SITE 3 - APPROXIMATE GAIN AS A FUNCTION OF PERCENT OF OBSERVATIONS IN THE CUMULATIVE DISTRIBUTION FUNCTIONS (CDF) FOR TOWED-ARRAY BEAM NOISE FOR AN ARRAY HEADING OF 135° WHEN ONE (AMBIGUOUS) SIDE OF THE ARRAY IS SUPPRESSED BY 30 dB.
Results for sidelobe suppression of 18, 26 and 35 dB. Array heading of 135°.

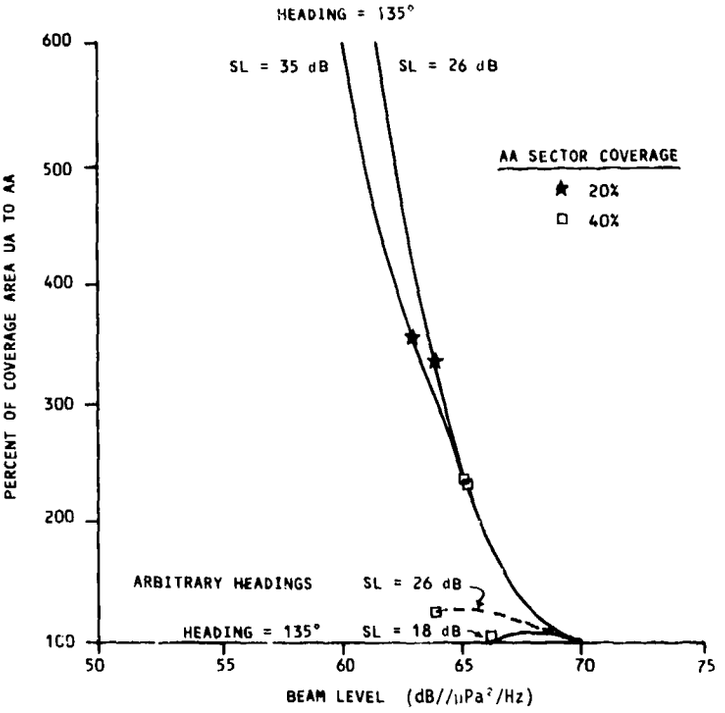

FIG. 20 SITE 3
INCREASE IN PERCENT OF AREA COVERAGE IN THE CUMULATIVE DISTRIBUTION FUNCTIONS FOR AN UNAMBIGUOUS TOWED ARRAY (UA) OVER AN AMBIGUOUS ARRAY (AA) FOR A HEADING OF 135° AND THREE LEVELS OF SIDELOBE SUPPRESSION.

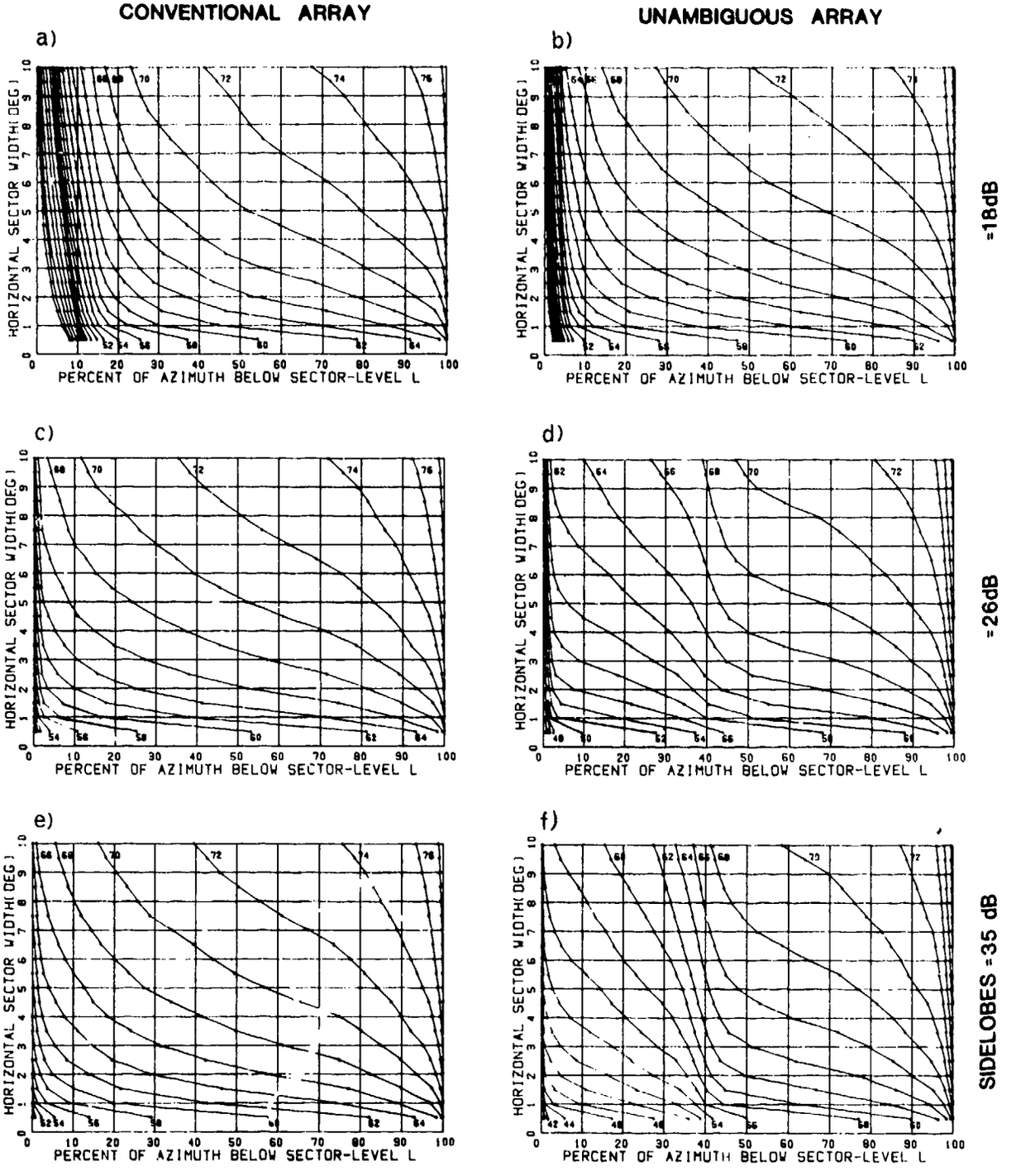

FIG. 21 SITE 4 - AACDF PLOTS
left-hand column conventional array
right-hand column left/right discriminating array with 18 dB (top row), 26 dB (centre row) and 35 dB (bottom row) sidelobe suppression. Array heading of 135°.

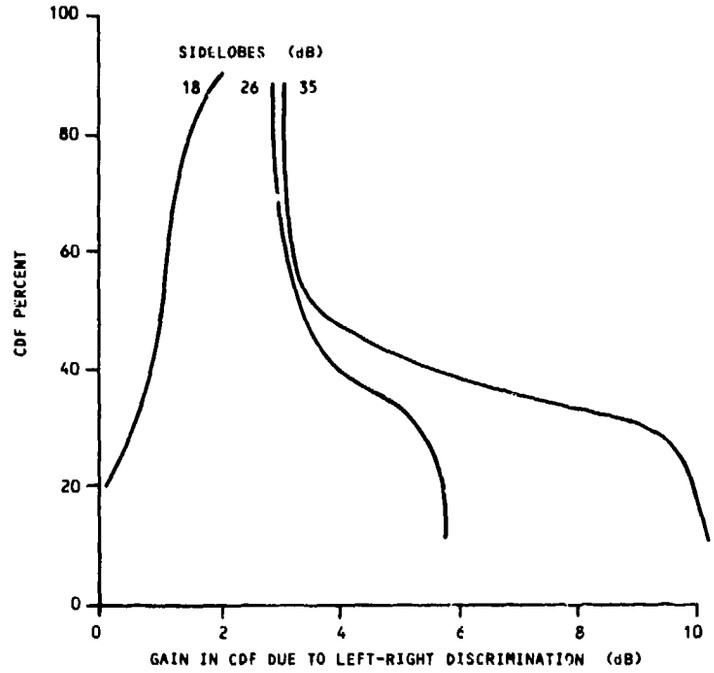

FIG. 22 SITE 4 - APPROXIMATE GAIN AS A FUNCTION OF PERCENTAGE OF OBSERVATIONS IN THE CUMULATIVE DISTRIBUTION FUNCTIONS (CDF) FOR TOWED-ARRAY BEAM NOISE FOR AN ARRAY HEADING OF 135° WHEN ONE (AMBIGUOUS) SIDE OF THE ARRAY IS SUPPRESSED 30 dB. Results for sidelobe suppression of 18, 26 and 35 dB. Array heading of 135°.

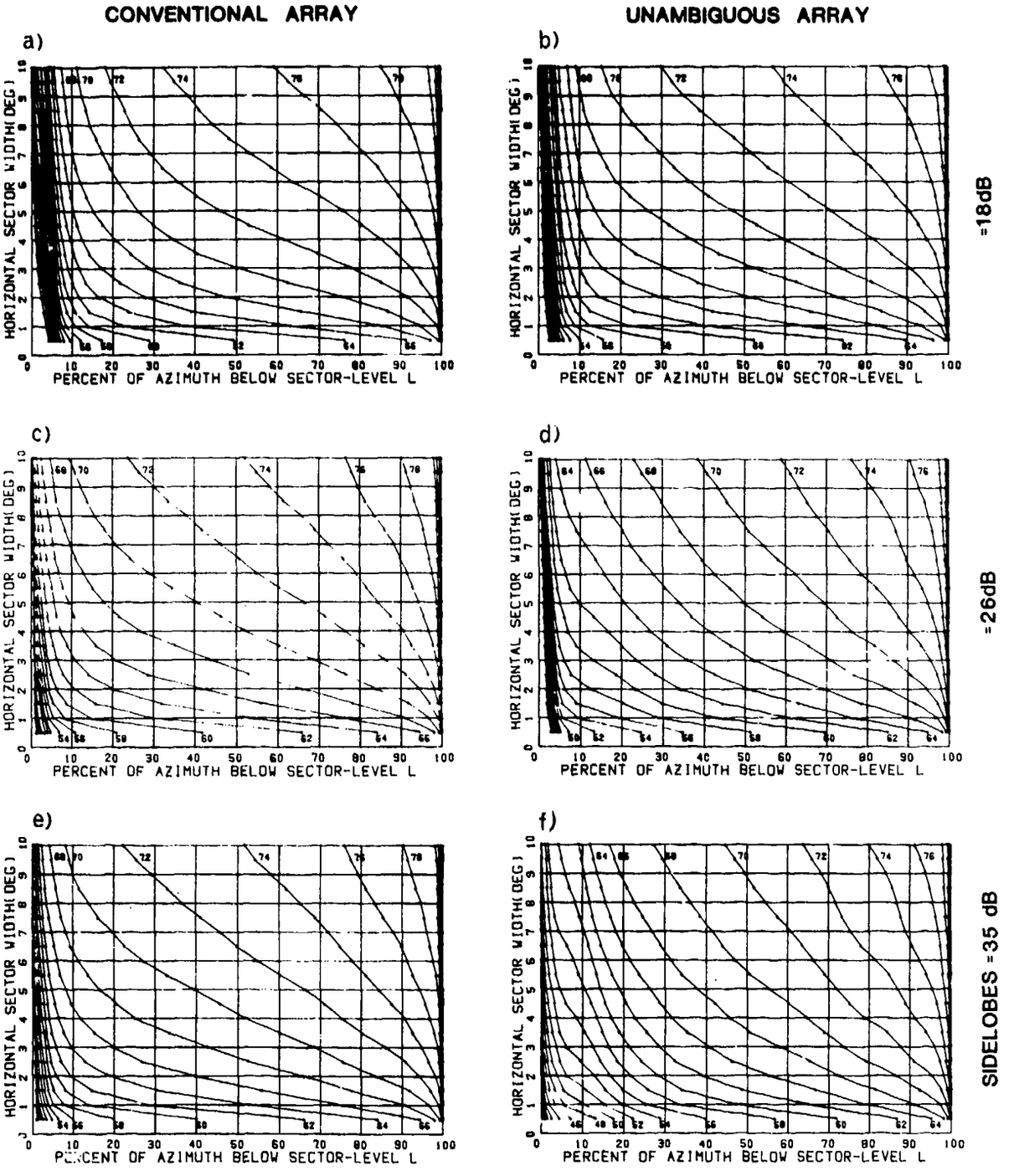

FIG. 23 SITE 5 - AACDF PLOTS
left-hand column conventional array
right-hand column left/right discriminating array with 18 dB (top row), 26 dB (centre row) and 35 dB (bottom row) sidelobe suppression. Array heading arbitrary.

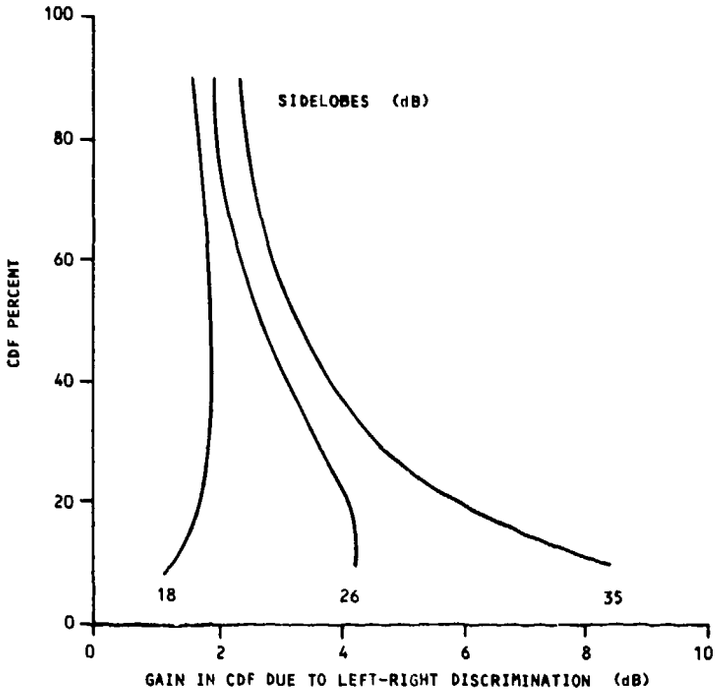

FIG. 24 SITE 5 - APPROXIMATE GAIN AS A FUNCTION OF PERCENTAGE OF OBSERVATIONS IN THE CUMULATIVE DISTRIBUTION FUNCTIONS (CDF) FOR TOWED-ARRAY BEAM NOISE FOR AN ARRAY HEADING OF 135° WHEN ONE (AMBIGUOUS) SIDE OF THE ARRAY IS SUPPRESSED BY 30 dB. Results for sidelobe suppression of 18, 26 and 35 dB. Array heading arbitrary.

APPENDICES

APPENDIX A

MODEL SENSITIVITY

When a study uses a model in which many assumptions are made to simplify the problem, there are always questions about the affects of those assumptions on the results. Some of these questions can be partially answered by performing a limited number of laborious operations, without the simplicity afforded by the assumptions or by the modelling "shortcuts". One obvious question concerns the affect on the AACDF plots of using a smooth curve for transmission loss instead of using a more complex calculation involving range and azimuth dependence.

In previous work, Site 5 was divided into nine azimuthal sectors in which different bathymetry profile, bottom-loss equation, and sets of sound-speed profiles were used for each sector. A range-dependent ray-theory calculation was made for the propagation loss versus range in each sector. These results were then used to generate the noise field, with all other parameters remaining the same as in the other present study. The AACDF results for the four principal quadrants are included in Fig. A.1(a-d). Horizontal-directionality estimates from averaged output of an unambiguous 11°-wide with 20 and 28 dB sidelobes are also included in Fig. A.1. The corresponding AACDF results for a single propagation loss (PL) equation of the form $PL = 69 + 15 \log R(\text{kyd}) + \alpha R(\text{in dB})$, where α is an attenuation coefficient, are given in Fig. 3 of the main text. Figure B.1 (Site 5, Column 1) contains the corresponding directionality plot for 26 dB sidelobes (Fig. B.2 is also for this site).

Comparison of noise-field quadrant AACDFs for the two cases indicates that the more complex ray-theory approach gives a greater distribution of levels. The high levels are about the same but the lower levels are not as well represented in the results for the smoothed propagation loss. Such a result would suggest that the spatial gains achievable from left/right discrimination are better than the AACDF plots in this study indicate. This is due to the gain increasing with the lower percentages of beam-noise levels. Since the high levels are produced with about the same frequency of occurrence by both approaches, the high-level end of the cumulative distribution functions (CDF) are about the same. For the lower levels, the CDFs are spread out more in the case of the more complex propagation-loss calculation. The region of improved performance at the lower end of the CDFs will be correspondingly extended. Hence the expected spatial gain resulting from left/right discriminating elements in a towed array could be several decibels more than the figures herein indicate. However, as the sidelobe suppression capability of the array decreases, the differences in the noise-field resolution become less important. At a suppression level of 26 dB, which is perhaps a practical upper limit for towed arrays, the lower end of the distribution gets cut off. The lower end of the CDFs would be artificially shifted toward higher levels eliminating the low beam-levels that might have been achieved as a result of the more variable propagation-loss values obtained with a ray-theory calculation of propagation loss.

When the noise directionality plots for the more complex ray-theory propagation-loss calculation in Fig. B.1 (for 20 and 28 dB sidelobe

suppression levels) are compared with the analogous results in Figs. B.1 (Site 5, lefthand column) and B.2 (dotted and solid curves for 26 and 35 dB sidelobes, respectively), it is evident that the noise-field directionality is relatively insensitive to the form of the propagation calculation. The omnidirectional levels were also reasonably insensitive. For the more complicated calculation the mean level was 88.1 dB, with a standard deviation for the fifteen measurement periods of 1.65 dB. The corresponding results for the simple propagation-loss equation were 88.8 dB and 0.65 dB respectively (see Fig.3 of the main text). A loss of about one decibel in standard deviation is not considered significant when a change of 5 to 15 dB along an individual azimuth is a common occurrence.

Additional factors of importance are the vertical arrival structure and array tilt. These have the effect of spreading the noise energy in azimuth and reducing the range of the beam-noise levels. This is illustrated by selected beam-noise plots in Fig. A.2. The light curves are for beam noise measured at Site 5 on six different headings at different times. In this case, the array is assumed to be horizontal and the noise field has no vertical-arrival structure. The heavy curves are for the same periods but with the noise having the same vertical structure as in the present study and an array tilt of 6°. These are the same plots as for the conventional array in Fig. 2 of the main text for measurement periods 2, 4, 6, 7, 8, and 12. Comparison of the two curves in each plot of Fig. A.2 indicates that the azimuthal smoothing due to a vertical-arrival structure in the noise field and a tilted array lowers the higher beam levels slightly and raises the lower levels considerably. The net effect on the CDFs of the beam-noise levels will be to lower the highest levels observed and to bias the lower end of the distribution upwards by eliminating the lowest values and decreasing the frequency of occurrence of the moderately low levels. For the particular case illustrated by Fig. A.2, it is obvious that the AACDFs for the realistic case of a noise field with a vertical-arrival structure and a tilted array should be considerably different from those for the ideal case of a horizontal array in a horizontal noise field. The AACDFs calculated for these two cases, on the other hand, do not differ significantly. The dashed curves in the Plot of Fig. A.3 for a vertical-arrival structure and a tilted array do not vary more than one decibel from the corresponding results, in solid curves, for a horizontal array and a flat noise field. The differences between the two sets of curves are only a fraction of a decibel except, near the centre of the plot, where they approach one decibel. This indicates that the deconvolution process in WIT successfully removes most of the spatial smoothing of the array. The filtering, which is then performed on the deconvolved-folded noise field, does not have vertical structure or array tilt. Hence very little difference is seen between the two.

The implication of this, for the present study, is that the AACDFs for the tilted array will be artificially biased to lower levels with a greater range of levels than would be expected. The use of a smoothed curve of propagation loss versus range instead of a more realistic one, however, has the effect of biasing the AACDFs to higher levels, cutting off the low levels. These two effects are opposite and partially cancel each other. How close they are to being equal is not known. However, the combined effect is not considered serious in the present study. If exact values are critical to a given analysis, the results herein should be redone with a more realistic propagation-loss calculation and using noise-field vertical structure and array tilt in the calculations for the AACDFs.

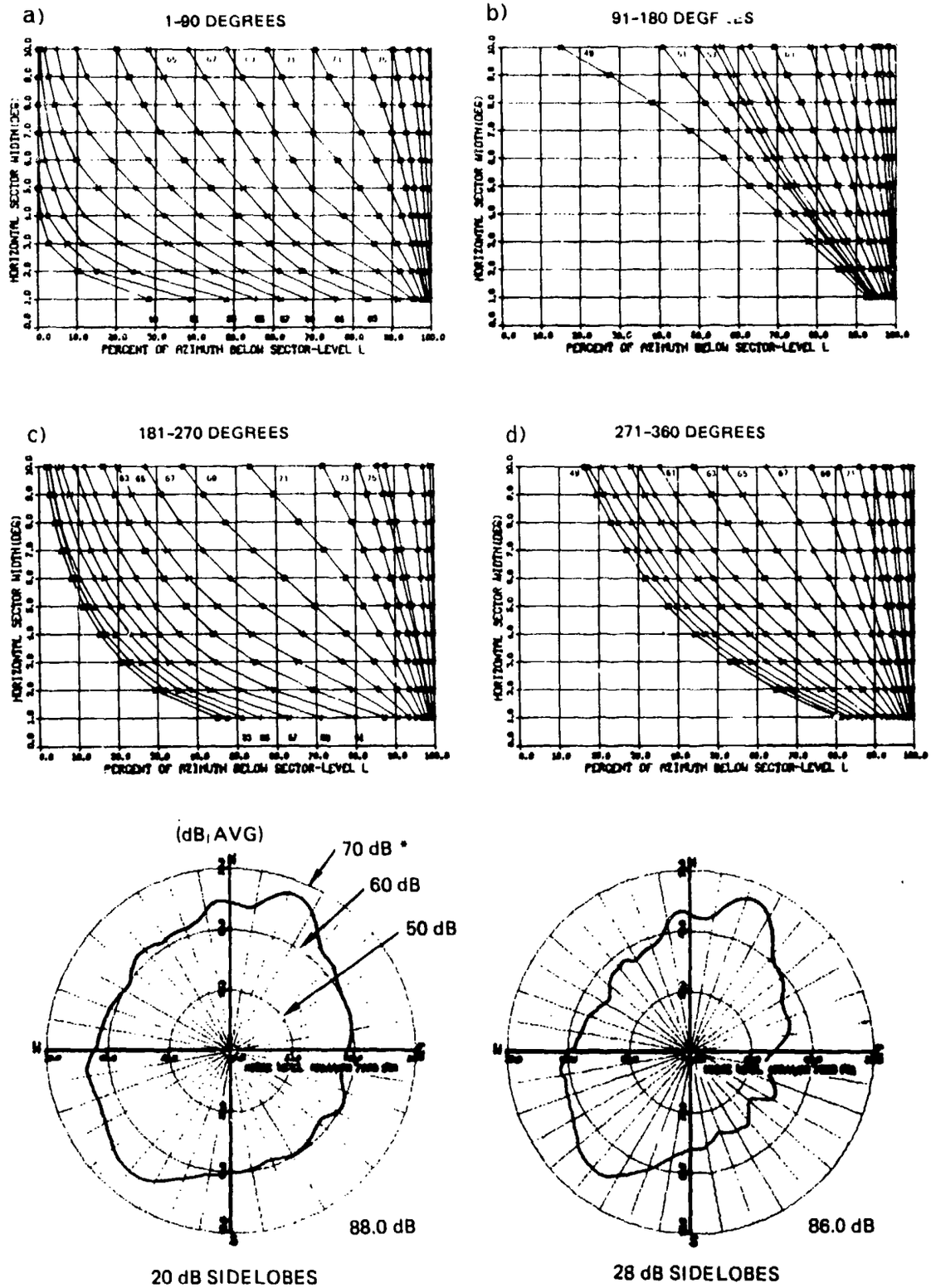

FIG. A.1 SITE 5 - NOISE-FIELD QUADRANT AACDF PLOTS AND HORIZONTAL DIRECTIONALITY ESTIMATED FROM AVERAGED OUTPUT OF AN 11° WIDE UNAMBIGUOUS BEAM WHEN THE SITE IS DIVIDED INTO SECTORS AND RANGE-DEPENDANT RAY THEORY IS USED TO CALCULATE THE PROPAGATION LOSS.

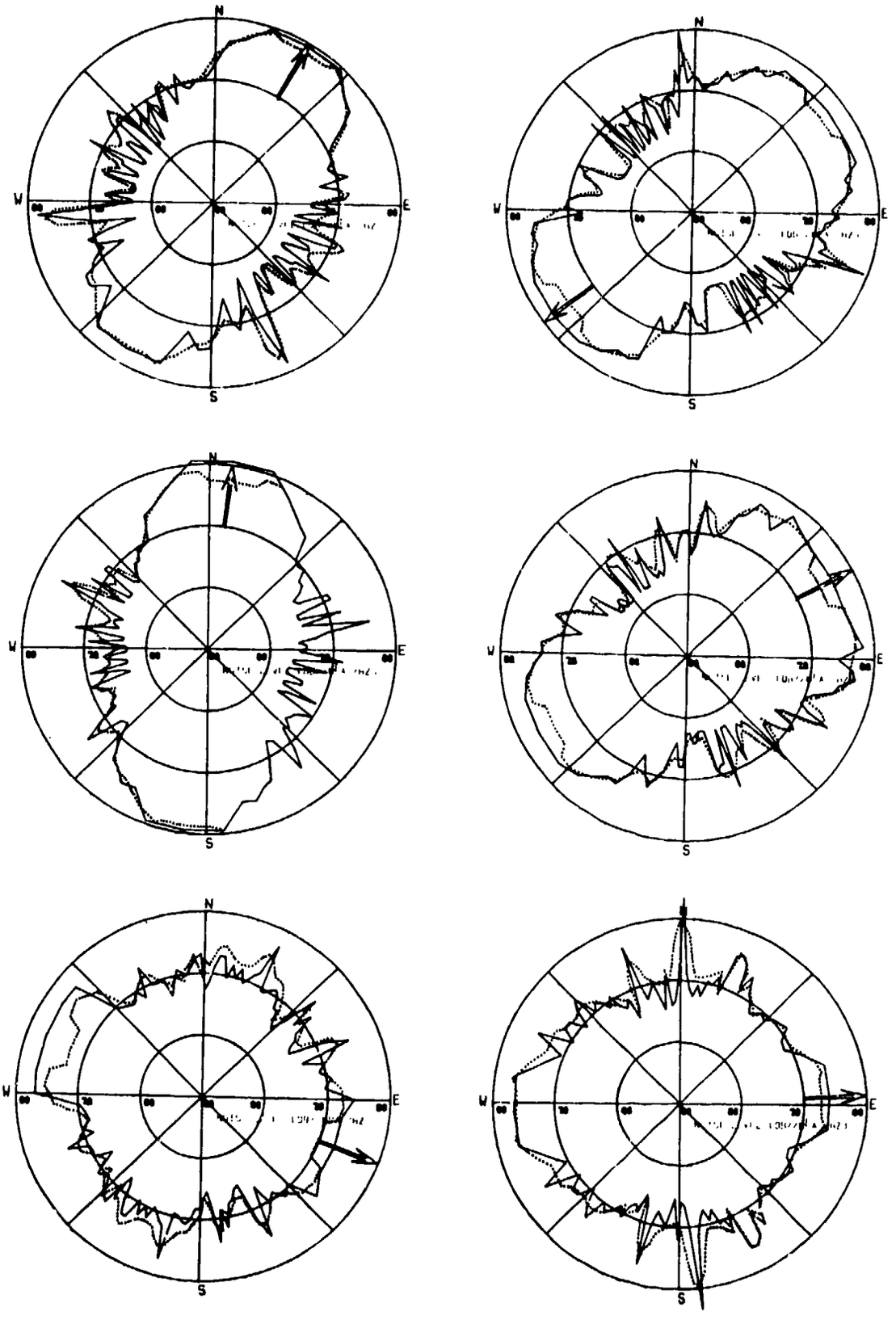

FIG. A.2 SITE 5 - SELECTED BEAM-OUTPUT DATA FOR A CONVENTIONAL ARRAY
solid curve noise field without vertical-arrival structure horizontal array
dotted curve noise field with vertical-arrival structure array tilt 6°
Sidelobes suppressed by 26 dB.

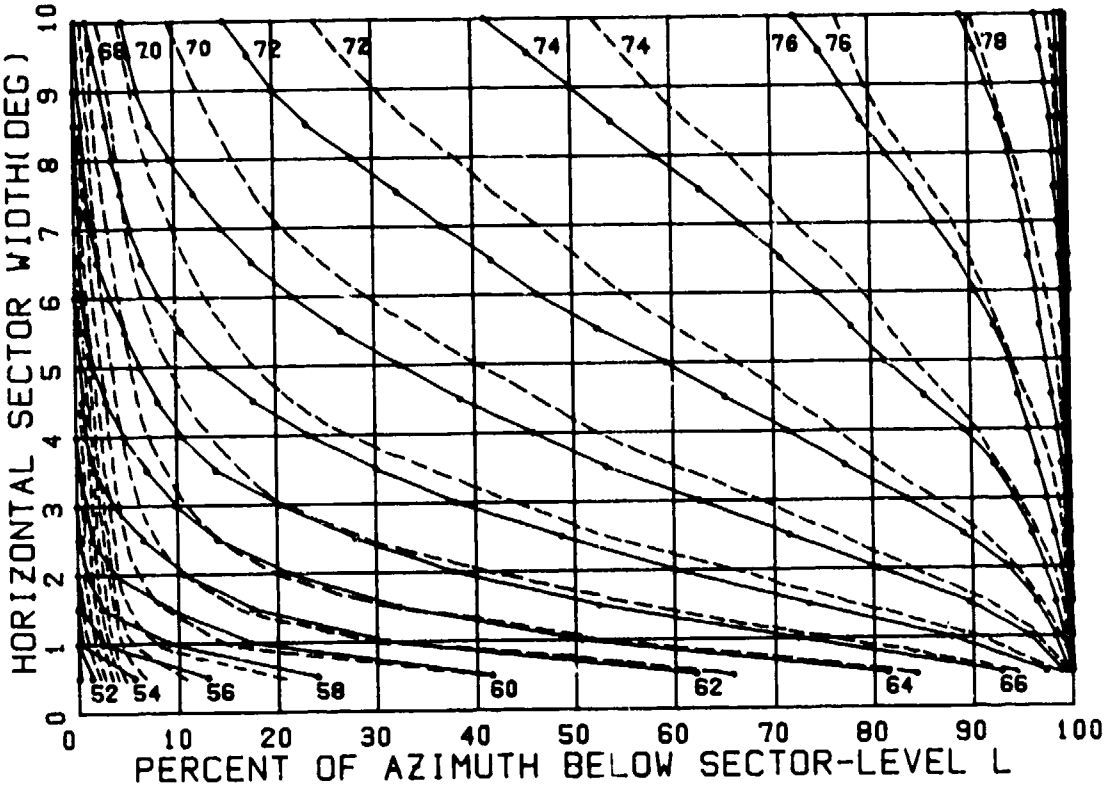

FIG. A.3 *SITE 5 - AACDF PLOTS FOR BEAM-NOISE LEVELS OF A CONVENTIONAL TOWED ARRAY ON AN ARBITRARY HEADING*

solid curve — *noise field without vertical-arrival structure horizontal array*

dotted curve — *noise field with vertical-arrival structure array tilt 6°*

Sidelobes are suppressed by 26 dB.

APPENDIX B

AMBIENT-NOISE HORIZONTAL DIRECTIONALITY AT EACH SITE

The horizontal directionality of the ambient noise was obtained for each of the six measurement sites. This was done in two different ways. The first was to smooth the "spike" field with a $[\sin x/x]^2$ filter of 5° between half-power points and 26 dB uniform sidelobes outside the main-beam response. The resulting 360 levels, one for each degree of azimuth were averaged over 15 periods, each separated by 1½ hours (21½ hr total). No ambiguity exists in these data; hence, none needs to be resolved. The result is an estimate of the average per-degree noise level as a function of azimuth. The second approach was to use Wagstaff's iterative technique (WIT) <B.1> to estimate the horizontal directionality from the array beam noise levels (including vertical-arrival structure and array tilt) obtained for the fifteen different measurements (on different headings) at each site. The results of both of these approaches are given in Fig. B.1. The left-hand column contains the results of the per-degree averaged output of the 5°-wide unambiguous beam. The right-hand column contains the WIT results. The results for each site are in order of the rows, i.e. Site 1 results in Row 1, Site 2 results in Row 2, etc.

Comparison of the two columns of directionality plots supports three conclusions. The first is that the WIT result is a good estimator of the unambiguous per-degree average for a corresponding beam (or smoothing filter) width. Along most azimuths, the two plots for a given site are in agreement within about one decibel. The second conclusion is that the WIT result achieves lower levels in some of the low-level directions. This is a result of some of the sidelobe contamination being removed by WIT. Hence, WIT is a better estimator in the low azimuth directions. This is illustrated by Fig. B.2 in which the WIT result for 26 dB sidelobe level (dashed curve) and the per-degree averaged 5°-wide unambiguous beam outputs for 26 dB (dotted curve) and 35 dB sidelobes (solid curve) are superimposed. Along the directions of low-level noise the WIT result (dashed curve) agrees better with the unambiguous 5°-wide beam per-degree averaged output for 35 dB sidelobe suppression level (solid curve) than does the corresponding one for 26 dB sidelobes (dotted curve). This indicates that the low levels estimated by WIT are probably better estimates of the noise in the directions of low-level noise than are the per-degree averaged unambiguous beam outputs for the same side-lobe suppression level.

REFERENCE

B.1 WAGSTAFF, R.A. Horizontal directionality estimation considering array tilt and noise field vertical-arrival structure. Journal of the Acoustical Society of America 67(4), 1980: 1287-1294.

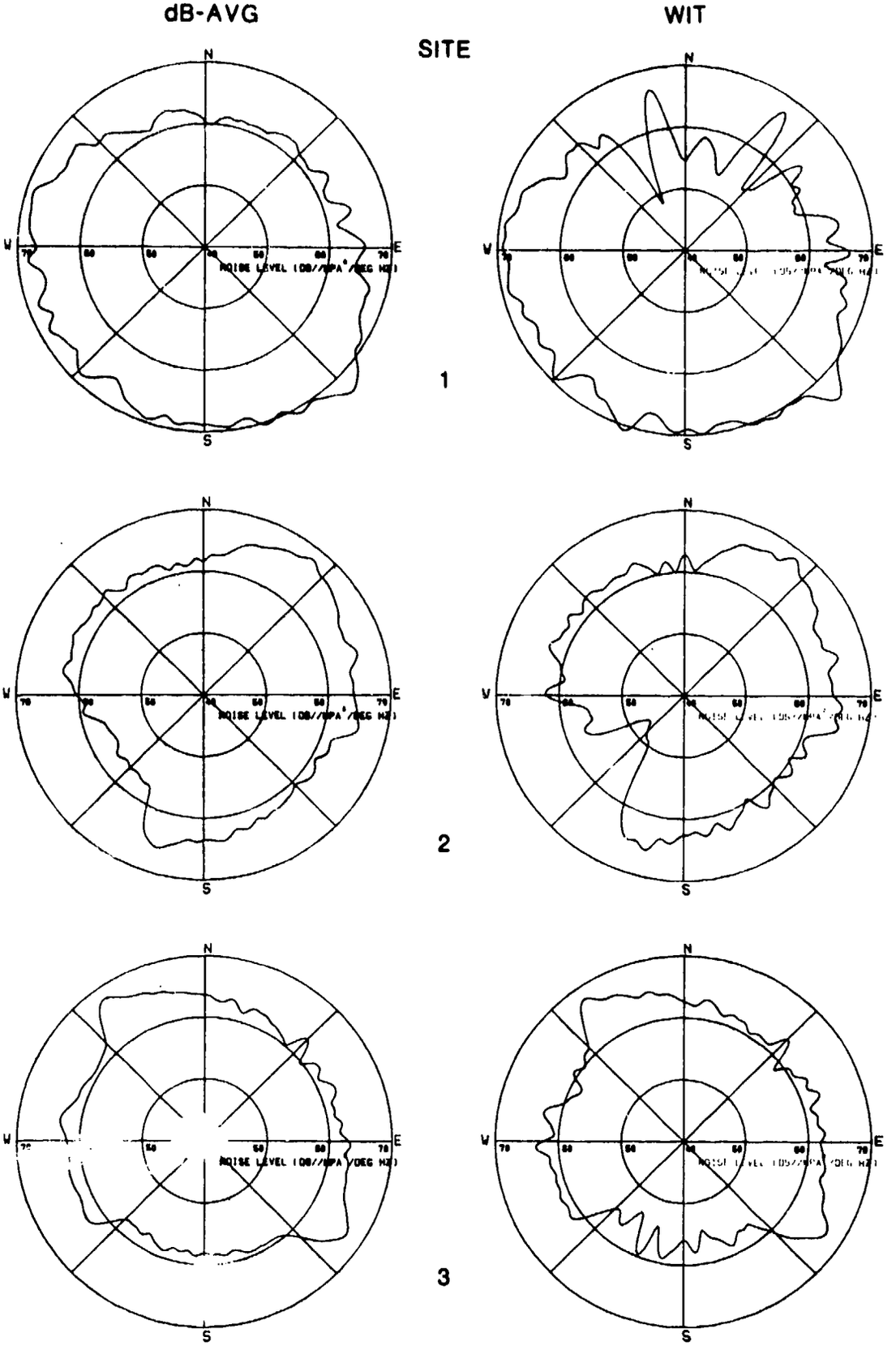

FIG. B.1 HORIZONTAL DIRECTIONALITY OF THE AMBIENT NOISE AT EACH SITE
left-hand column determined from the geometric mean (dB-AVG) of the unambiguous beam of 5° width and 26 dB sidelobes
right-hand column corresponding estimate from the conventional array beam-noise levels using Wagstaff's Iterative Technique (WIT).

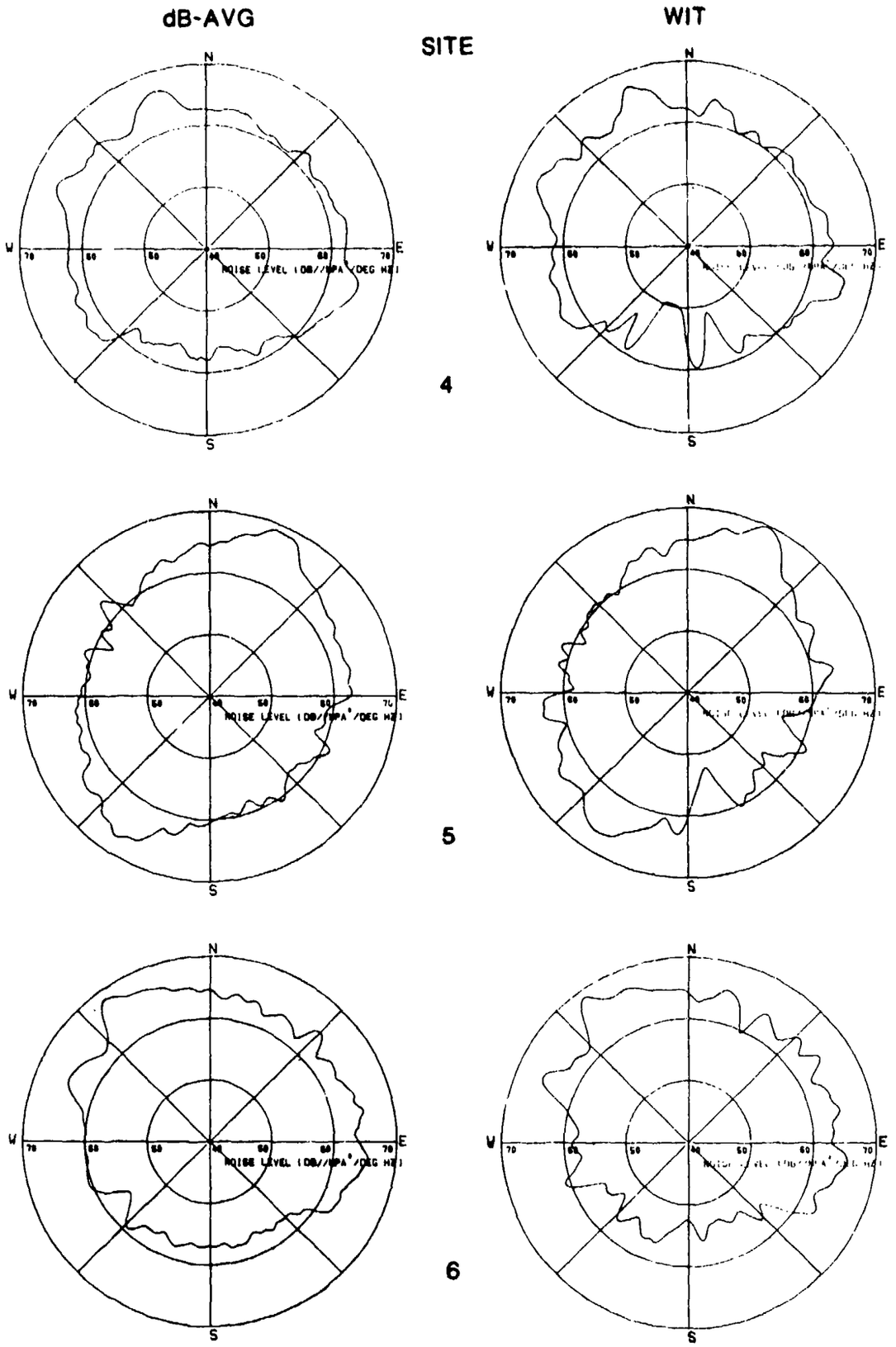

FIG. B.1 (Cont'd) HORIZONTAL DIRECTIONALITY OF THE AMBIENT NOISE AT EACH SITE
left-hand column determined from the geometric mean (dB-AVG) of the unambiguous beam of 5° width and 26 dB sidelobes
right-hand column corresponding estimate from the conventional array beam-noise levels using Wagstaff's Iterative Technique (WIT).

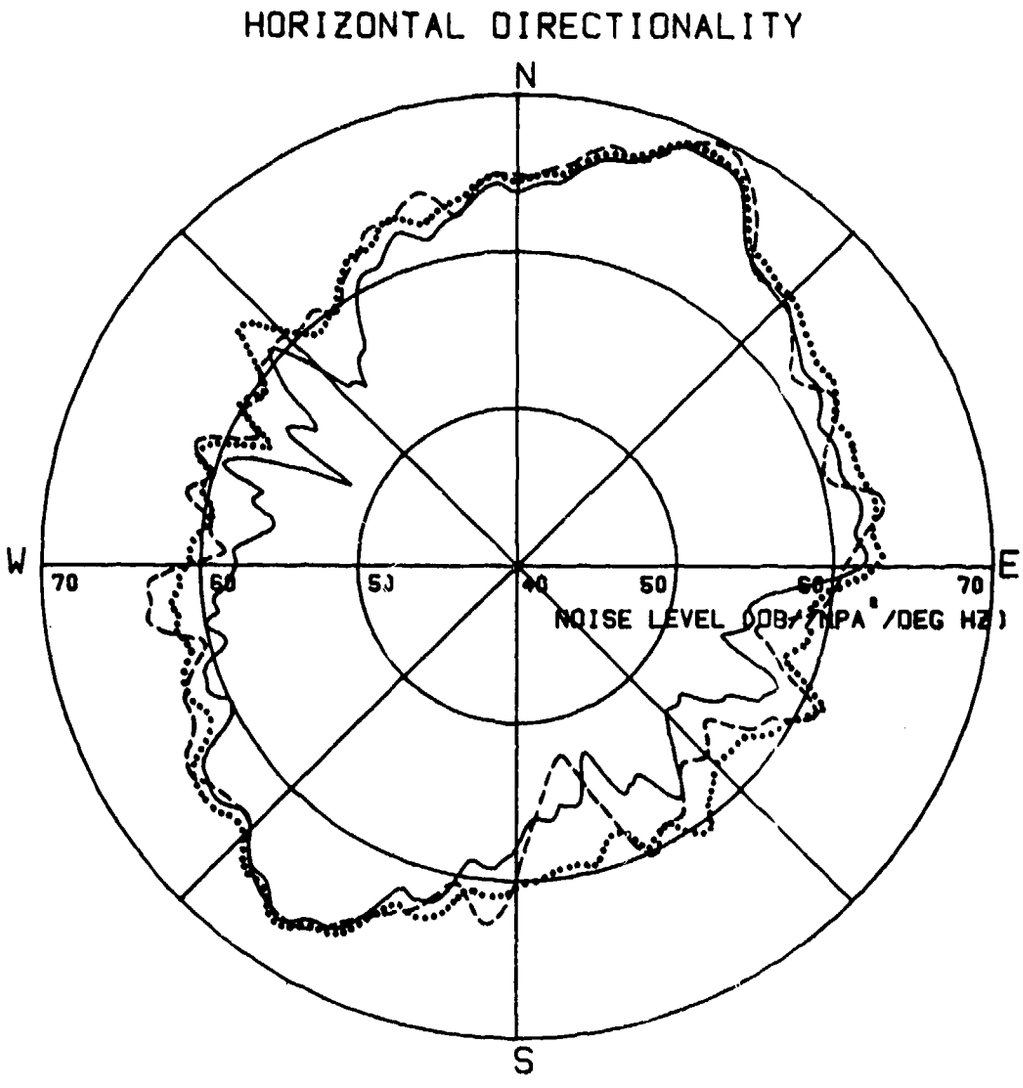

FIG. B.2 SITE 5 - AMBIENT-NOISE HORIZONTAL DIRECTIONALITY FROM A 5° WIDE UNAMBIGUOUS BEAM WITH 35 dB (solid curve) AND 26 dB (dotted curve) SIDELOBES AND FROM WIT (dashed curve) WITH 26 dB SIDELOBES.